

AFWL-TR-75-153

AFWL-TR-
75-153

2

ADA020310

STRONGLY PHASE-ABERRATED NONDIFFRACTION LIMITED LASER BEAMS

Charles B. Hogge

January 1976



Final Report

Approved for public release; distribution unlimited.

**AIR FORCE WEAPONS LABORATORY
Air Force Systems Command
Kirtland Air Force Base, NM 87117**

FEB 9 1976

This final report was prepared by the Air Force Weapons Laboratory, under Job Order Number 33260996, Kirtland Air Force Base, New Mexico. Mr. C.B. Hogge (ALO) was the Laboratory Project Officer-in-Charge.

When US Government drawings, specifications, or other data are used for any purpose other than a definitely related Government procurement operation, the Government thereby incurs no responsibility nor any obligation whatsoever, and the fact that the Government may have formulated, furnished, or in any way supplied the said drawings, specifications, or other data is not to be regarded by implication or otherwise as in any manner licensing the holder or any other person or corporation or conveying any rights or permission to manufacture, use, or sell any patented invention that may in any way be related thereto.

This report has been reviewed by the Information Office (OI) and is releasable to the National Technical Information Service (NTIS). At NTIS, it will be available to the general public, including foreign nations.

This technical report has been reviewed and is approved for publication.

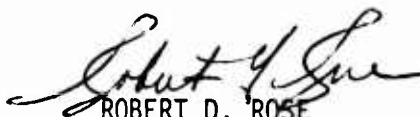


CHARLES B. HOGGE
Project Officer

FOR THE COMMANDER



ARMAND D. MAIO
Lt. Colonel, USAF
Chief, Optics Branch



ROBERT D. ROSE
Colonel, USAF
Chief, Advanced Laser Technology Division



DO NOT RETURN THIS COPY. RETAIN OR DESTROY.

UNCLASSIFIED

SECURITY CLASSIFICATION OF THIS PAGE (When Data Entered)

REPORT DOCUMENTATION PAGE		READ INSTRUCTIONS BEFORE COMPLETING FORM
1. REPORT NUMBER 14 AFWL-TR-75-153	2. GOVT ACCESSION NO.	3. RECIPIENT'S CATALOG NUMBER
4. TITLE (and Subtitle) 6 STRONGLY PHASE-ABERRATED NONDIFFRACTION LIMITED LASER BEAMS.	5. TYPE OF REPORT & PERIOD COVERED 9 Final Report.	
6. AUTHOR 10 Charles B. Hogge	7. PERFORMING ORG. REPORT NUMBER	
8. CONTRACT OR GRANT NUMBER(s)		
9. PERFORMING ORGANIZATION NAME AND ADDRESS Air Force Weapons Laboratory (ALO) Kirtland Air Force Base, NM 87117		10. PROGRAM ELEMENT, PROJECT, TASK AND SUB-PROJECT INIT NUMBERS 62601F 33260996
11. CONTROLLING OFFICE NAME AND ADDRESS Air Force Weapons Laboratory Air Force Systems Command Kirtland Air Force Base, NM 87117		12. REPORT DATE 11 January 1976
14. MONITORING AGENCY NAME & ADDRESS (if different from Controlling Office)		13. NUMBER OF PAGES 12 68 p.
16 AF-3326 17 332609		15. SECURITY CLASS. (of this report) Unclassified
15a. DECLASSIFICATION/DOWNGRADING SCHEDULE		
16. DISTRIBUTION STATEMENT (of this Report) Approved for public release; distribution unlimited.		
17. DISTRIBUTION STATEMENT (of the abstract entered in Block 20, if different from Report)		
18. SUPPLEMENTARY NOTES		
19. KEY WORDS (Continue on reverse side if necessary and identify by block number) Propagation Nondiffraction limited Aberrations Random phase <i>(SIGMA SQUARED SUB L)</i> <i>(-4 PI SQUARED SIGMA SQUARED SUB L)</i>		
20. ABSTRACT (Continue on reverse side if necessary and identify by block number) Both amplitude and phase aberrations usually alter and reduce the intensity of the focal plane distribution of an optical system. Phase fluctuations are generally the more important; if the square root of the ensemble averaged phase variance (σ_ϕ^2) is less than 0.1 wavelength, the reduction in maximum irradiance is given quite well by $\exp[-4\pi^2 \sigma_\phi^2]$ almost without regard to the correlation size of the phase fluctuation. For larger phase distortions, this simple formula will predict a very severe intensity reduction that may be		


CONT. 116

UNCLASSIFIED

SECURITY CLASSIFICATION OF THIS PAGE(When Data Entered)

(B1k 20)

much too pessimistic. In this situation, a careful accounting of the influence of the relative size of the phase correlation length is necessary for an accurate prediction of the intensity reduction. It can be shown, then, that the irradiance profile of the strongly phase aberrated beam can be written approximately as the direct sum of two beams, the respective characteristics of which depend on the phase variance and correlation length.



UNCLASSIFIED

CONTENTS

<u>Section</u>		<u>Page</u>
I	INTRODUCTION	5
II	EFFECT OF STRONG PHASE DISTORTIONS AND FINITE PHASE CORRELATION LENGTHS	9
III	SOME OBSERVATION APPROPRIATE TO THE RANDOM PHASE SCATTERING PROCESS	32
	Exact Solution	35
	Simplified Quantitative Results for Strongly Phase Aberrated Nondiffraction Limited Beams	36
IV	SYSTEM JITTER AND CASCADED RANDOM PHASE DISTORTIONS	53
	System Jitter	53
	Cascaded Random Phase Distortions	54
V	OPTICAL SYSTEM MODELS	60
VI	CONCLUSIONS	65

ILLUSTRATIONS

<u>Figure</u>		<u>Page</u>
1	Reduction in Relative Maximum Average Irradiance for Various Amounts of rms Phase Distortion (σ_ℓ) Versus the Ratio of the Transmitter Spot Size to the Phase Correlation Length	12
2	Relative Irradiance Profiles for Different Amounts of rms Phase Distortion (σ_ℓ) Versus the Relative Phase Correlation Length	
	(a) $\sigma_\ell = 0.1$ wavelength	13
	(b) $\sigma_\ell = 0.2$ wavelength	14
	(c) $\sigma_\ell = 0.3$ wavelength	15
	(d) $\sigma_\ell = 0.4$ wavelength	16
	(e) $\sigma_\ell = 0.5$ wavelength	17
3	Integrated Relative Power Profiles for the Same Cases Shown in Figure 2	
	(a) $\sigma_\ell = 0.1$ wavelength	18
	(b) $\sigma_\ell = 0.2$ wavelength	19
	(c) $\sigma_\ell = 0.3$ wavelength	20
	(d) $\sigma_\ell = 0.4$ wavelength	21
	(e) $\sigma_\ell = 0.5$ wavelength	22
4	Relative Accuracy of the First Order Prediction for the Maximum Average Irradiance for Various Phase Distortions (σ_ℓ) and Relative Phase Correlation Length (ω_t/ℓ_0)	23
5	Relative Accuracy of the Second Order Prediction for the Maximum Average Irradiance for Various Phase Distortions (σ_ℓ) and Relative Phase Correlation Length (ω_t/ℓ_0)	24
6	Ratio of Second Order to First Order Prediction for the Maximum Average Irradiance for $\sigma_\ell = 0.1$ and 0.2 wavelength Versus the Relative Phase Correlation Length (ω_t/ℓ_0)	25
7	N is the Number of Times Diffraction Limited that the Focal Plane Irradiance Distribution Becomes When One Uses Power in a Fixed Bucket as the Definition	
	(a) N^2 versus (ω_t/ℓ_0)	26
	(b) N^2 versus (σ_ℓ)	27
8	Typical Modulation Transfer Function for a Random Phase Distortion Decomposed into Two Separate Functions	34
9	Typical Far-Field Irradiance Profile of a Phase Aberrated Non-diffraction Limited Beam Composed of the Sum of $I_u(r)$ and $I_s(r)$	40

ILLUSTRATIONS (Continued)

<u>Figure</u>		<u>Page</u>
10	Reduction in Relative Maximum Average Irradiance Using the Modified Two Gaussian Beam Model with the Different Approximations for the Scale Size L for Different rms Phase Distortions and Relative Correlation Lengths (ω_t/ℓ_0)	
	(a) L_1 scale approximation	42
	(b) L_2 scale approximation	43
	(c) L_3 scale approximation	44
11	Reduction in Relative Maximum Average Irradiance Using the Modified Two Gaussian Beam Model with the Exact Calculation for the Scale Size L for different rms Phase Distortions and Relative Correlation Lengths (ω_t/ℓ_0)	45
12	Ratio of the Exact Calculation for the Maximum Average Irradiance to the Modified Two Gaussian Beam Calculation as a Function of Phase Distortion (σ_ℓ) and Relative Correlation Length (ω_t/ℓ_0)	46
13	Dependence of Relative Scale Size (L/ℓ_0) on the rms Phase Distortion σ_ℓ	47
14	Relative Irradiance Profiles for Different Amounts of rms Phase Distortion and Relative Phase Correlation Length (ω_t/ℓ_0) as Calculated using the Modified Two Gaussian Beam Model	
	(a) $\sigma_\ell = 0.1$ wavelength	48
	(b) $\sigma_\ell = 0.2$ wavelength	49
	(c) $\sigma_\ell = 0.3$ wavelength	50
	(d) $\sigma_\ell = 0.4$ wavelength	51
	(e) $\sigma_\ell = 0.5$ wavelength	52
15	Cascaded MTF for Two Processes, One with a Very Small Phase Correlation Length and One with a Much Larger Correlation Length	58
16	Parametric Dependence of M on the Relative Intensity Reduction and the Relative Integrated Power Decrease	59
17	Three Approximations to the Nondiffraction Limited Beam	63

SECTION I

INTRODUCTION

The focal plane irradiance distribution of a phase aberrated beam with a small phase correlation length can be well represented as the incoherent sum of two beams, as discussed in reference 1. One of the beams consists of the ideal diffraction limited beam scaled by an attenuation factor $\exp(-\sigma_\phi^2)$, where

$$\sigma_\phi^2 = 4\pi^2 \sigma_\ell^2 \quad (1)$$

and

$$\sigma_\ell^2 = \left(\frac{\overline{\ell^2}}{\lambda^2} \right) \quad (2)$$

$\overline{\ell^2}$ is the time averaged variance of the optical path length fluctuations, λ is the optical wavelength. The quantity σ_ℓ is conveniently used to describe the "number of waves" of distortion; for instance, for a root mean square (rms) distortion of a tenth of a wave, $\sigma_\ell = 0.1$ and $\sigma_\phi^2 \approx 0.4$.

The second beam, which can contain a large fraction of the total energy, is related to the shape of the power spectrum of the phase fluctuations; in the case where the phase correlation length is small compared to the aperture diameter, the on-axis irradiance of this beam is very small. Attendant with this, the beam is very large in lateral extent. Physically, this behavior is explained simply as wide angle scattering effect from the small scale phase inhomogeneities. This effect has been studied, for instance, in the investigation of photographic film grain characteristics (ref. 2).

Strictly speaking, the derivation leading to this "two beam" representation is only accurate when $\sigma_\phi^2 \leq 0.1$. Furthermore, one can neglect the contribution of the second beam only under conditions when $\ell_0 \ll \omega_t$, where ℓ_0 is the

-
1. Hogge, C.B., Butts, R.R., and Burlakoff, M., Applied Optics **13**, 1065, May 1974.
 2. Stark, H. Applied Optics **10**, 333, 1971.

correlation length of the phase fluctuation and ω_t is the output aperture radius. Nonetheless, when these conditions are satisfied, one can obtain a useful representation of the focal plane irradiance distribution of an optical system as

$$\langle I(r) \rangle = I_d(r) \exp(-\sigma_\phi^2) \quad (3)$$

where $I_d(r)$ is the irradiation distribution of the diffraction limited beam. In fact, for improved laser systems showing nearly diffraction limited operation, this representation of the laser irradiance distribution has been found to agree well with experimental observations*, a fact that lends some insight into the very nature of the residual phase distortions present in the lasers.

On the other hand, many laser systems operate with output characteristics that are strongly nondiffraction limited either for reasons associated with the laser design characteristics itself or perhaps for reasons related to the environment in which the system must operate. With σ_λ larger than a tenth of a wave, the expansion leading to the simple interpretation of reference and especially the representation suggested by equation (3), is no longer necessarily valid. In particular, it can be shown that under conditions where $\sigma_\lambda > 0.1$, the correlation length of the phase fluctuations becomes an important parameter in the complete description of the phase aberrated beam. Reference 1 alluded to this dependence in the description of the second beam generated by the scattering from the phase inhomogeneities. In fact, equation (3) is only valid for the single special case where the correlation of the phase distortions is much smaller than the system limiting aperture diameter. Retaining the first order expansion terms of equation (5), in reference 1, the influence of the finite correlation length can be seen to affect the far-field irradiance distribution through the covariance function, as

$$\langle I(r) \rangle = I_0(r) + I_1(r) \quad (4)$$

where

$$I_0(r) = \exp(-\sigma_\phi^2) I_d(r) \quad (5)$$

*Dr. David R. Dean, Air Force Weapons Laboratory, Kirtland AFB, New Mexico, private communication.

$$I_1(r) = \exp(-\sigma_\phi^2) \int_0^\infty M_d(r_0) C_\phi(r_0) J_0\left(\frac{kr_0 r}{f}\right) r_0 dr_0 \quad (6-a)$$

$$I_d(r) \equiv \int_0^\infty M_d(r_0) J_0\left(\frac{kr_0 r}{f}\right) r_0 dr_0 \quad (7)$$

where $M_d(r)$ is the aberration-free output Optical Transfer Function (OTF), $C_\phi(r)$ is the covariance function of the random phase fluctuations, f is the system focal length, and $k = 2\pi/\lambda$. $I_0(r)$ is seen to be precisely the irradiance distribution of equation (3); $I_0(r)$ will be large compared to $I_1(r)$ only when $\sigma_\lambda < 0.1$ and when $\ell_0 \ll \omega_1$, for under this latter condition $C_\phi(r) \ll M_d(r)$ for any non-zero value of the respective radial arguments. Evaluating the on-axis irradiance and taking $M_d(r)$ constant over the range of integration gives

$$I_1(0) = \exp(-\sigma_\phi^2) K \int_0^\infty C_\phi(r) r dr \quad (6-b)$$

where K is a constant depending on characteristics of the optical system, such as power, wavelength, and aperture diameter. The right hand side of equation (6-b) must become very small as the width of $C_\phi(r)$ decreases; therefore, $I_1(0)$ decreases with decreasing correlation length.

If $\sigma_\lambda < 0.1$, but ℓ_0 is not small compared to the system output aperture diameter, equations (4), (5), and (6) can be used to calculate a more accurate focal plane irradiance distribution than does equation (3). The rms wave distortion is necessarily constrained to be small because equation (4) is obtained through a series expansion of the Modulation Transfer Function (MTF) of the random phase aberrations (assumed in reference 1 to be a Gaussian random variable). In terms of the phase covariance function, the random phase aberration MTF is given by

$$M_p(r) = \exp\left(-\sigma_\phi^2 + C_\phi(r)\right) \quad (8)$$

The expansion used for equation (4) is then

$$M_p(r) \approx \left[\exp(-\sigma_\phi^2)\right] \left(1 + C_\phi(r)\right) \quad (9)$$

and because $C_{\phi}(r) \leq \sigma_{\phi}^2$, $0 \leq r \leq \infty$, the expansion will be accurate to within 10 percent as long as $\sigma_{\phi} \leq 0.1$ wavelength.

SECTION II

EFFECT OF STRONG PHASE DISTORTIONS AND FINITE PHASE CORRELATION LENGTHS

To investigate the influence of the phase correlation length under conditions of strong phase distortions ($\sigma_\ell > 0.1$), the expansion of equation (9) can be continued. The calculations are significantly simplified if the input optical field distribution is assumed to be Gaussian with radial spot size ω_t to the e^{-2} intensity point. Also assume for simplicity that the covariance function of the random phase distortions is of the form

$$C_\phi(r) = \sigma_\phi^2 \exp(-r^2/\ell_0^2) \quad (10)$$

The integral scale size (ref. 3) of the phase fluctuations is defined as

$$L_0 = \frac{\int_0^\infty C_\phi(r) dr}{C_\phi(0)} = \left(\frac{\sqrt{\pi}}{2}\right) \ell_0 \quad (11)$$

$$L_0 \approx \ell_0 \quad (12)$$

and is a frequently used measure of the correlation length of the phase fluctuations. These assumptions, though restrictive in form, still allow one to investigate dependence of the far-field irradiance distribution on the parameters of interest, σ_ℓ and ℓ_0 . Under these assumptions, the average focal plane irradiance is given by

$$\langle I(r) \rangle = \frac{I_0}{\omega_t^2} \exp(-\sigma_\phi^2) \int_0^\infty \exp(-r_0^2/2\omega_t^2) \exp(C_\phi(r)) J_0\left(\frac{krr_0}{f}\right) r_0 dr_0 \quad (13)$$

3. Tatarski, T.A., Wave Propagation in a Turbulent Medium, Trans. by R.A. Silverman, Dover Publications, Inc., New York.

where

$$I_0 = I_d(0) = \frac{2\pi \omega_t^2 P_0}{\lambda^2 f^2} \quad (14)$$

and

$P_0 \triangleq$ total output power.

By continuing the expansion of $M_p(r)$ in equation (9), it is easy to show that

$$\langle I(r) \rangle = \exp(-\sigma_\phi^2) I_0 \sum_{n=0}^{\infty} \frac{\sigma_\phi^{2n}}{n!} \left(\frac{1}{1+2nR^2} \right) \exp \left[-\frac{2r^2}{\omega_f^2} \cdot \left(\frac{1}{1+2nR^2} \right) \right] \quad (15)$$

where $R = \left(\frac{\omega_t}{\ell_0} \right)$, and $\omega_f = \left(\frac{\lambda f}{\pi \omega_t} \right)$ is the focal plane spot size of the diffraction limited Gaussian beam.

The average far-field irradiance distribution is seen to be the incoherent sum of Gaussian beams with spot size

$$\omega_n^2 = \omega_f^2 \cdot (1 + 2nR^2) \quad (16)$$

and amplitudes

$$A_n = \frac{\sigma_\phi^{2n}}{n!} \cdot \frac{1}{(1+2nR^2)} \quad (17)$$

These spot sizes increase monotonically with n while the amplitudes can initially increase, but they will ultimately decrease with increasing n .

Equation (15) reduces as it should to the following limiting forms:

$$\lim_{\ell_0 \rightarrow \infty} \langle I(r) \rangle = I_d(r) \quad (18)$$

and

$$\lim_{\ell_0 \rightarrow 0} \langle I(r) \rangle = \exp(-\sigma_\phi^2) I_d(r) \quad (19)$$

where

$$I_d(r) = I_0 \exp \left(-2r^2/\omega_f^2 \right) \quad (20)$$

The following useful power-in-the-bucket information can be obtained by integrating equation (15):

$$P(r) = P_0 \left\{ 1 - \exp(-\sigma_\phi^2) \sum_{n=0}^{\infty} \frac{\sigma_\phi^{2n}}{n!} \exp \left[-\frac{2r^2}{\omega_f^2} \frac{1}{(1+2nR^2)} \right] \right\} \quad (21)$$

The parametric dependencies of $\langle I(r) \rangle$ and $P(r)$ are shown in figures 1 through 7. The purpose of these figures is to define under what conditions equation (4) will yield an adequate solution for the irradiance distribution. Furthermore, in the case of strong phase fluctuations, $\sigma_\ell > 0.1$, it is of interest to know how a finite correlation length will affect the irradiance distribution.

In figure 1, the on-axis relative irradiance is plotted versus the ratio of the transmitter spot size to the phase correlation length. Thus, for large abscissa values, the irradiance should approach the limiting value $\exp(-\sigma_\phi^2)$. While this is the case, it is clear that for $\sigma_\ell > 0.1$, the intensity can be a strong function of the relative size of the correlation length ($R = \omega_t/\ell_0$). The dependence is stronger for larger values of σ_ℓ ; but even for $\sigma_\ell = 0.2$, a factor of approximately two difference in the peak intensity is observed for an $R = 1$ as compared to $R = 2$. Clearly for $\sigma_\ell > 0.1$, an accurate prediction of the maximum irradiance value can only be obtained if an estimate is known for the phase correlation length -- because the simple prediction of equation (3) is too pessimistic.

Figures 2(a) to (e) are plots of the irradiance profiles for different selections of the parameters σ_ℓ and R . For $R \ll 1$, the nature of the optical distortion is like simple beam jitter. This can be easily seen by noting that when $R \ll 1$, $C_\phi(r)$ can be approximated over the effective region of integration in equation (13) by a first order expansion in r , with the result that

$$\langle I(x_0, y_0) \rangle \approx \iint_{-\infty}^{\infty} M(x, y) \exp \left[-\frac{\sigma_\phi^2}{\ell_0^2} (x^2 + y^2) \right] \exp \left[-\frac{ik}{f} (xx_0 + yy_0) \right] dx dy \quad (22)$$

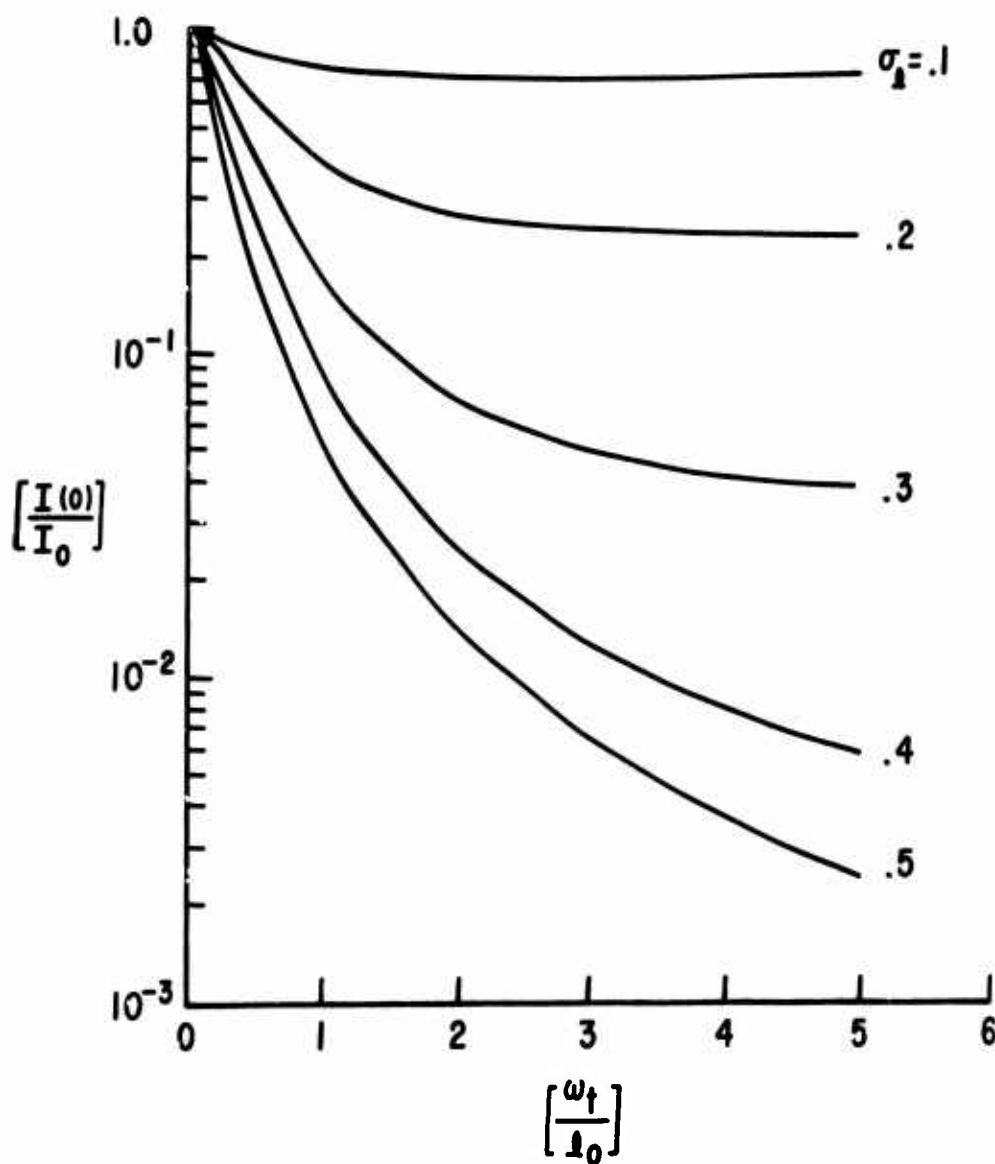
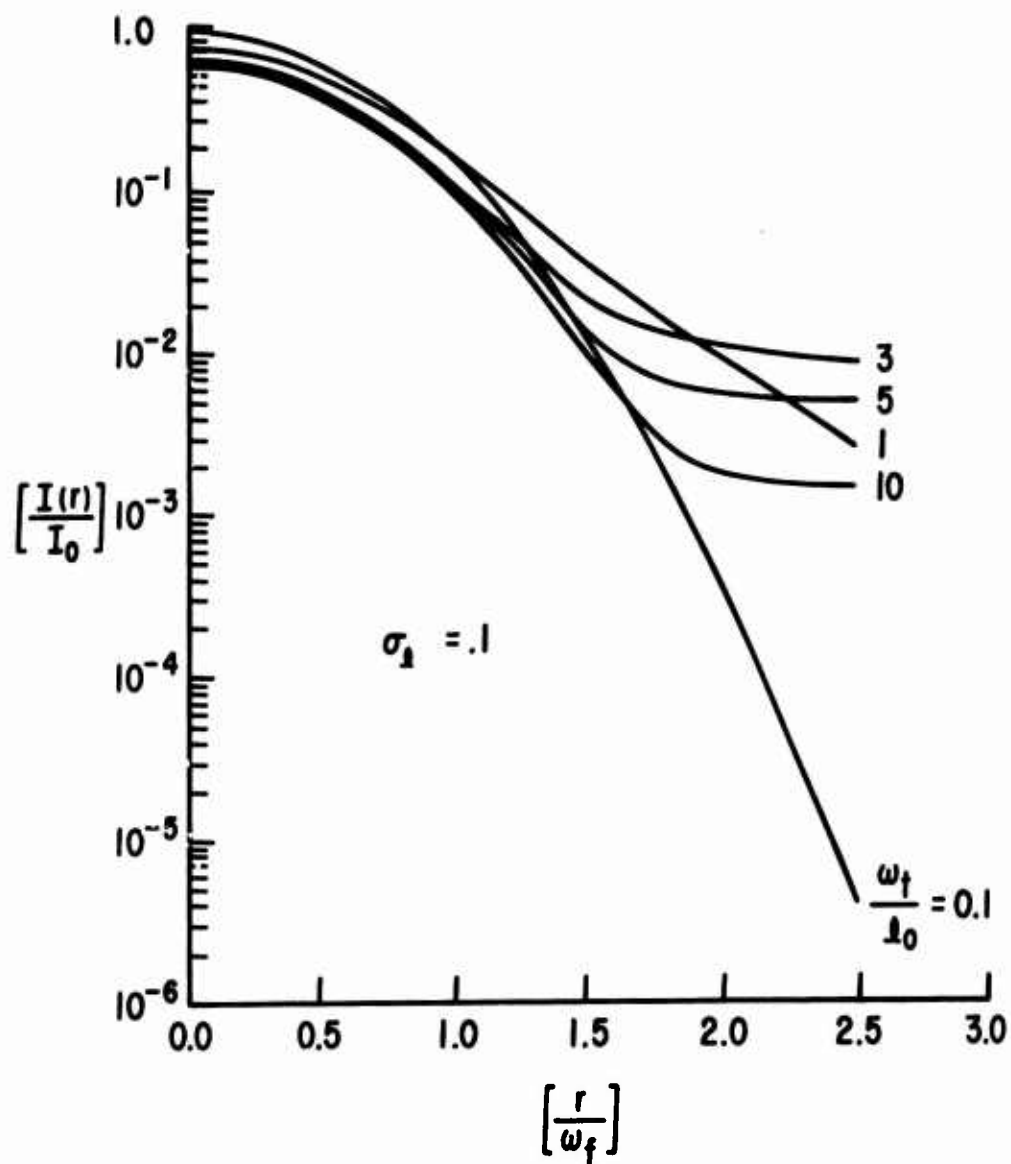
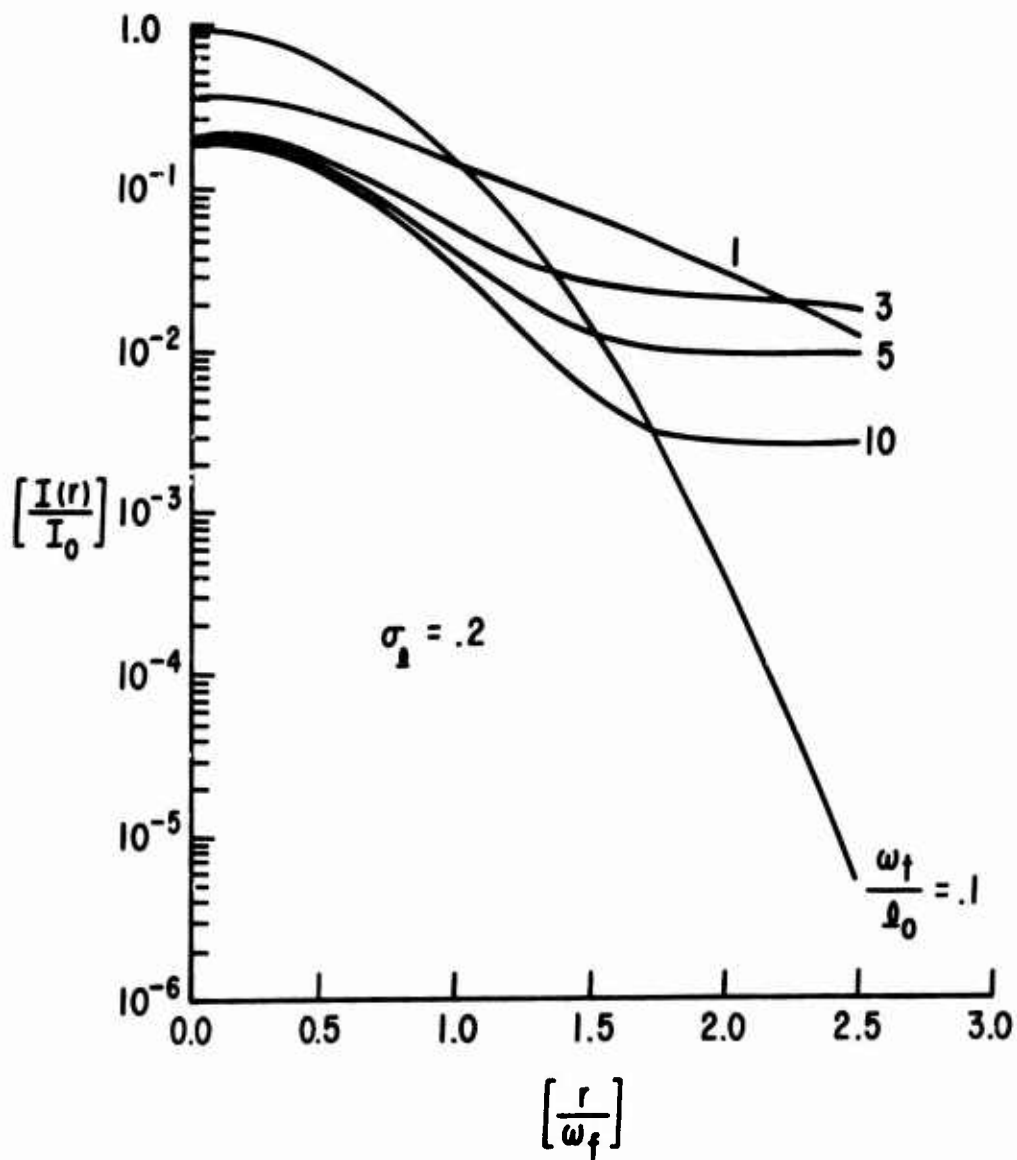


Figure 1. Reduction in Relative Maximum Average Irradiance for Various Amounts of rms Phase Distortion (σ_ϕ) Versus the Ratio of the Transmitter Spot Size to the Phase Correlation Length



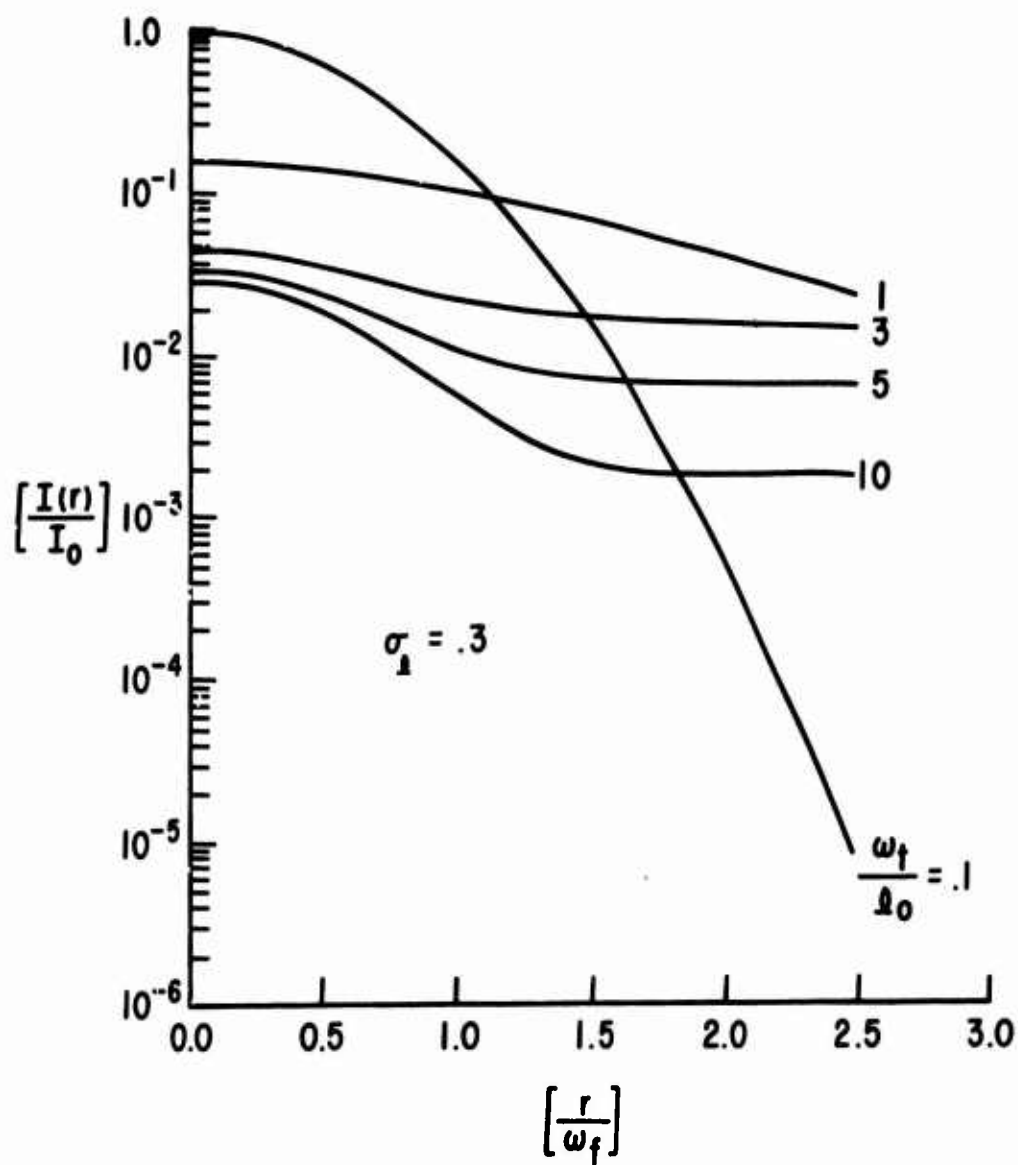
(a) $\sigma_\lambda = 0.1$ wavelength

Figure 2. Relative Irradiance Profiles for Different Amounts of rms Phase Distortion (σ_λ) Versus the Relative Phase Correlation Length



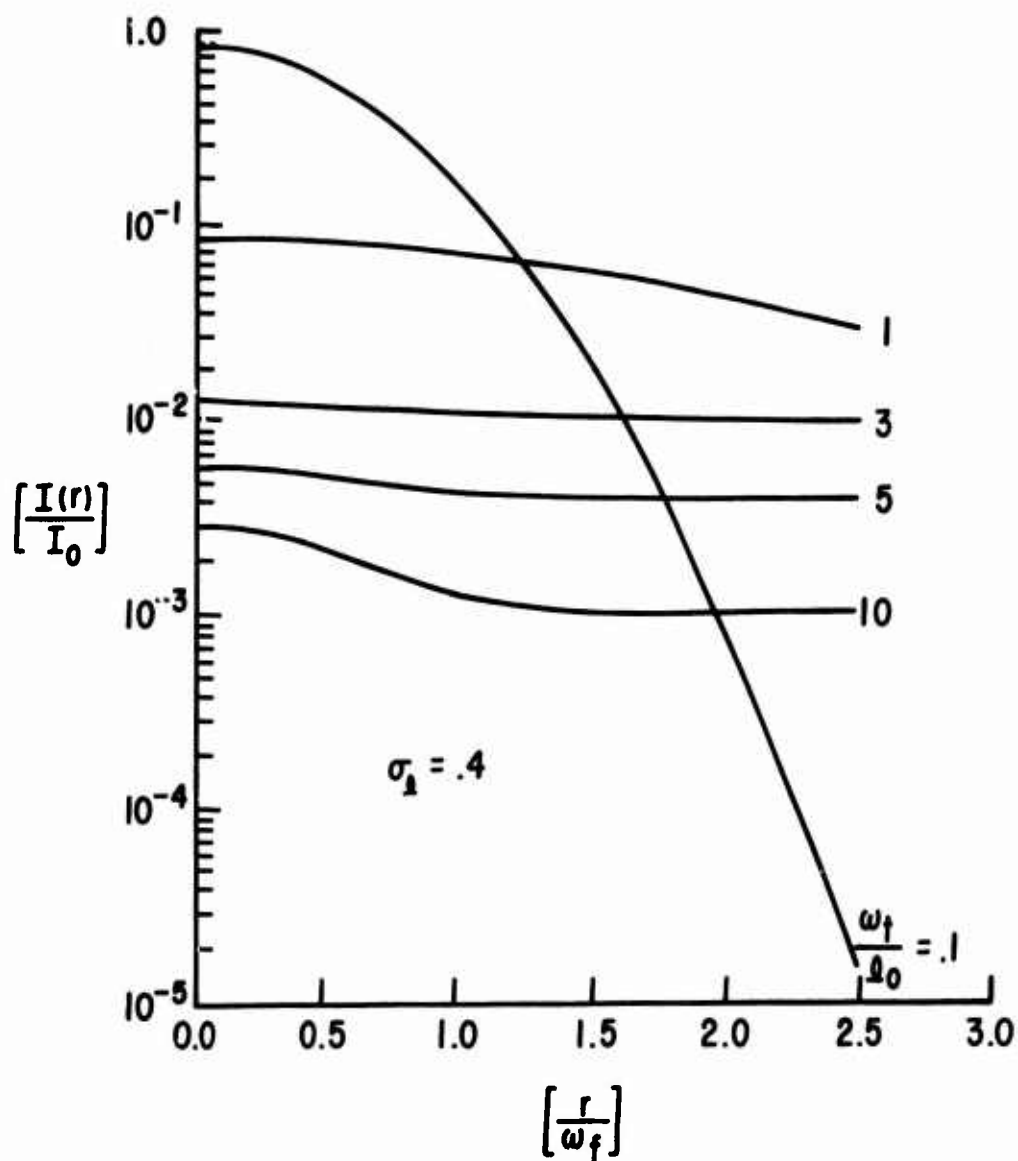
(b) $\sigma_\ell = 0.2$ wavelength

Figure 2. Relative Irradiance Profiles for Different Amounts of rms Phase Distortion (σ_ℓ) Versus the Relative Phase Correlation Length



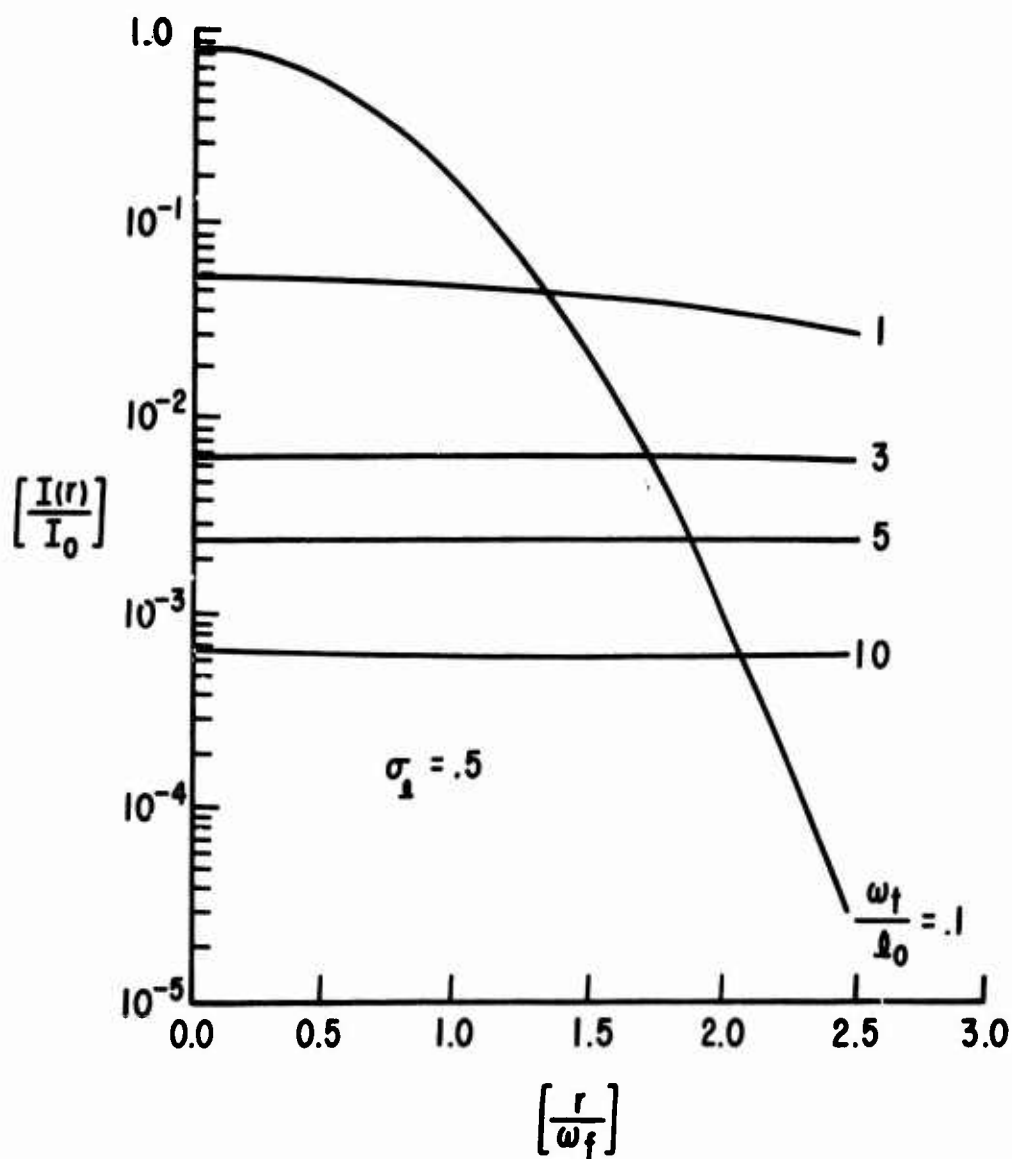
(c) $\sigma_\lambda = 0.3$ wavelength

Figure 2. Relative Irradiance Profiles for Different Amounts of rms Phase Distortion (σ_λ) Versus the Relative Phase Correlation Length



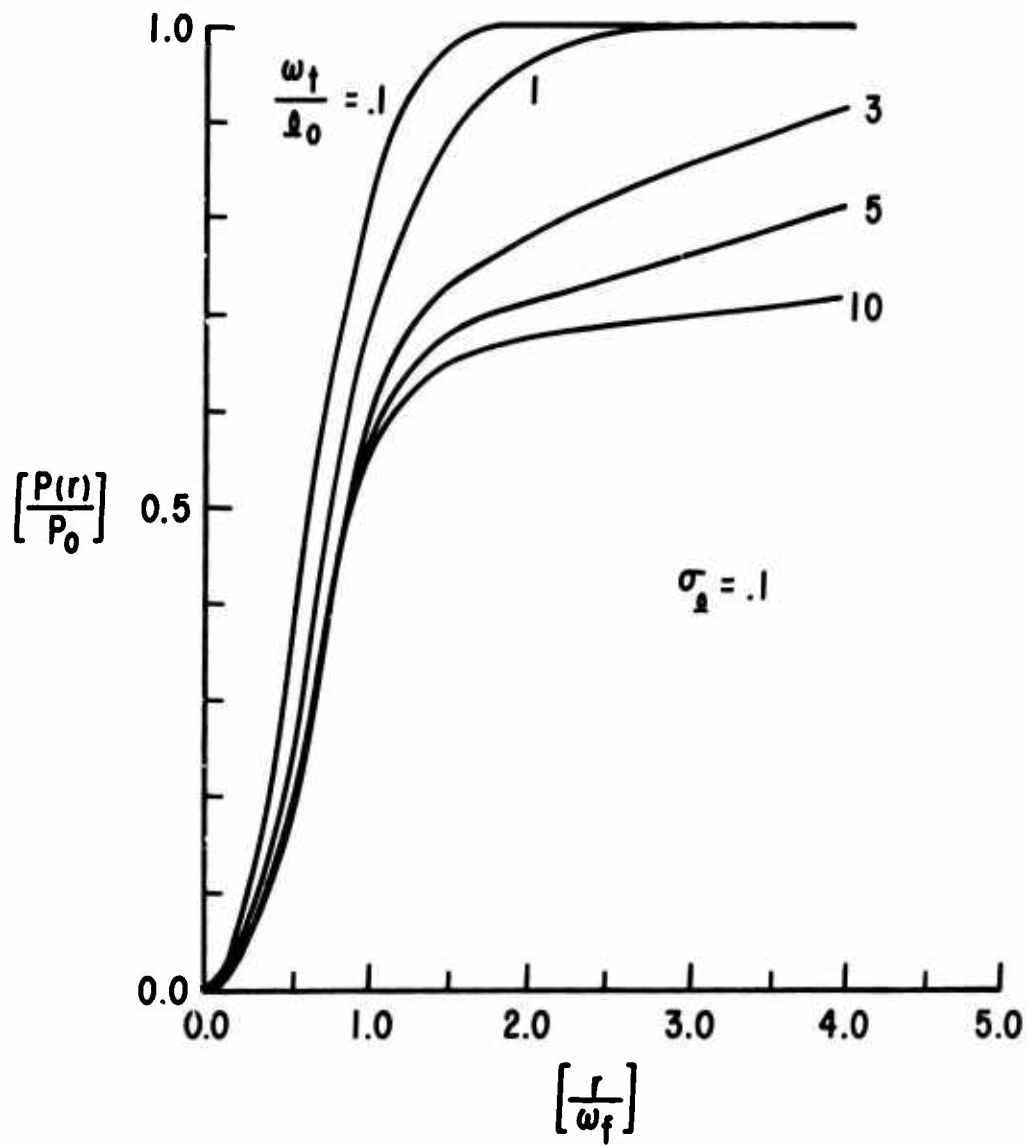
(d) $\sigma_\ell = 0.4$ wavelength

Figure 2. Relative Irradiance Profiles for Different Amounts of rms Phase Distortion (σ_ℓ) Versus the Relative Phase Correlation Length



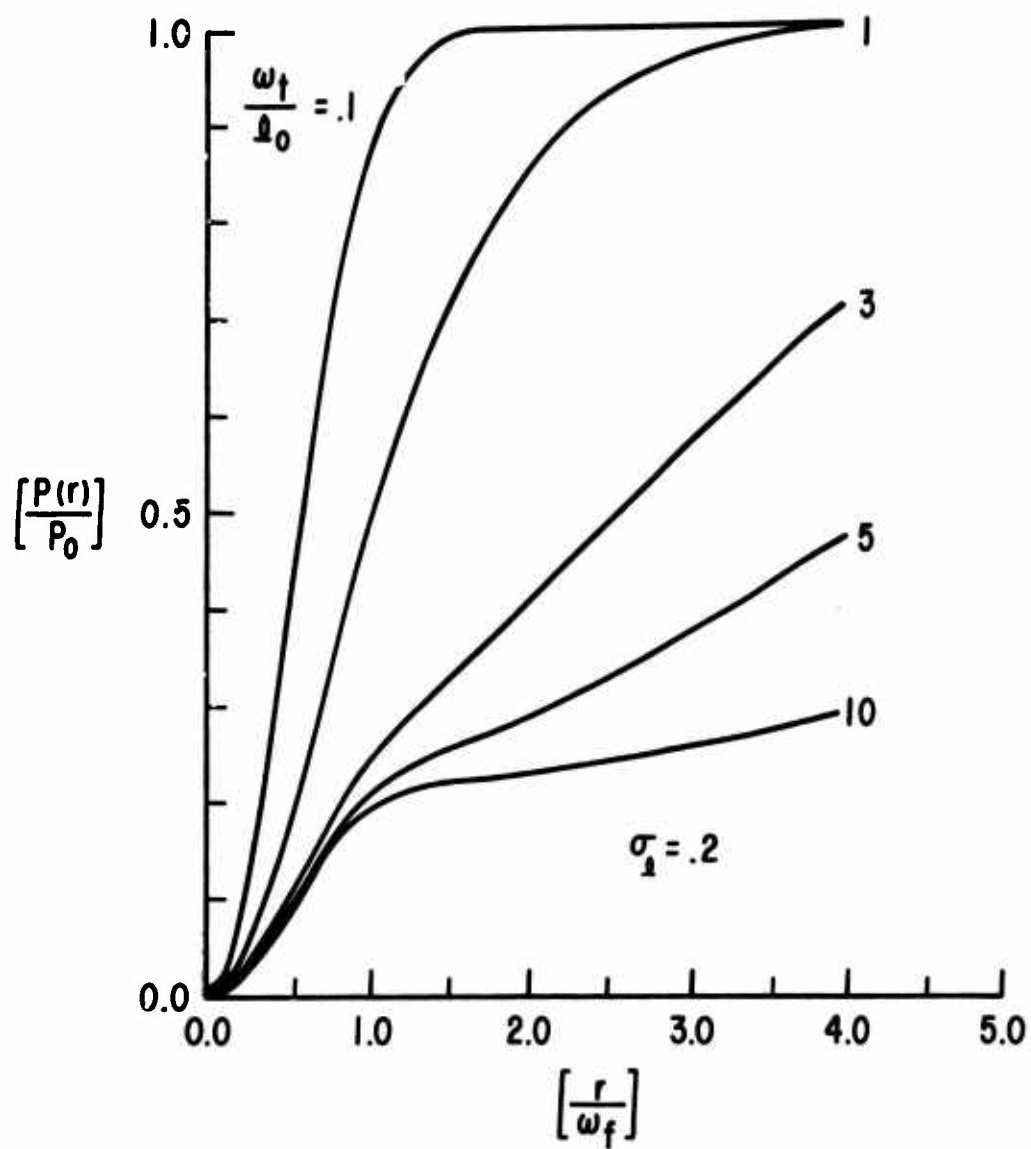
(e) $\sigma_\ell = 0.5$ wavelength

Figure 2. Relative Irradiance Profiles for Different Amounts of rms Phase Distortion (σ_ℓ) Versus the Relative Phase Correlation Length



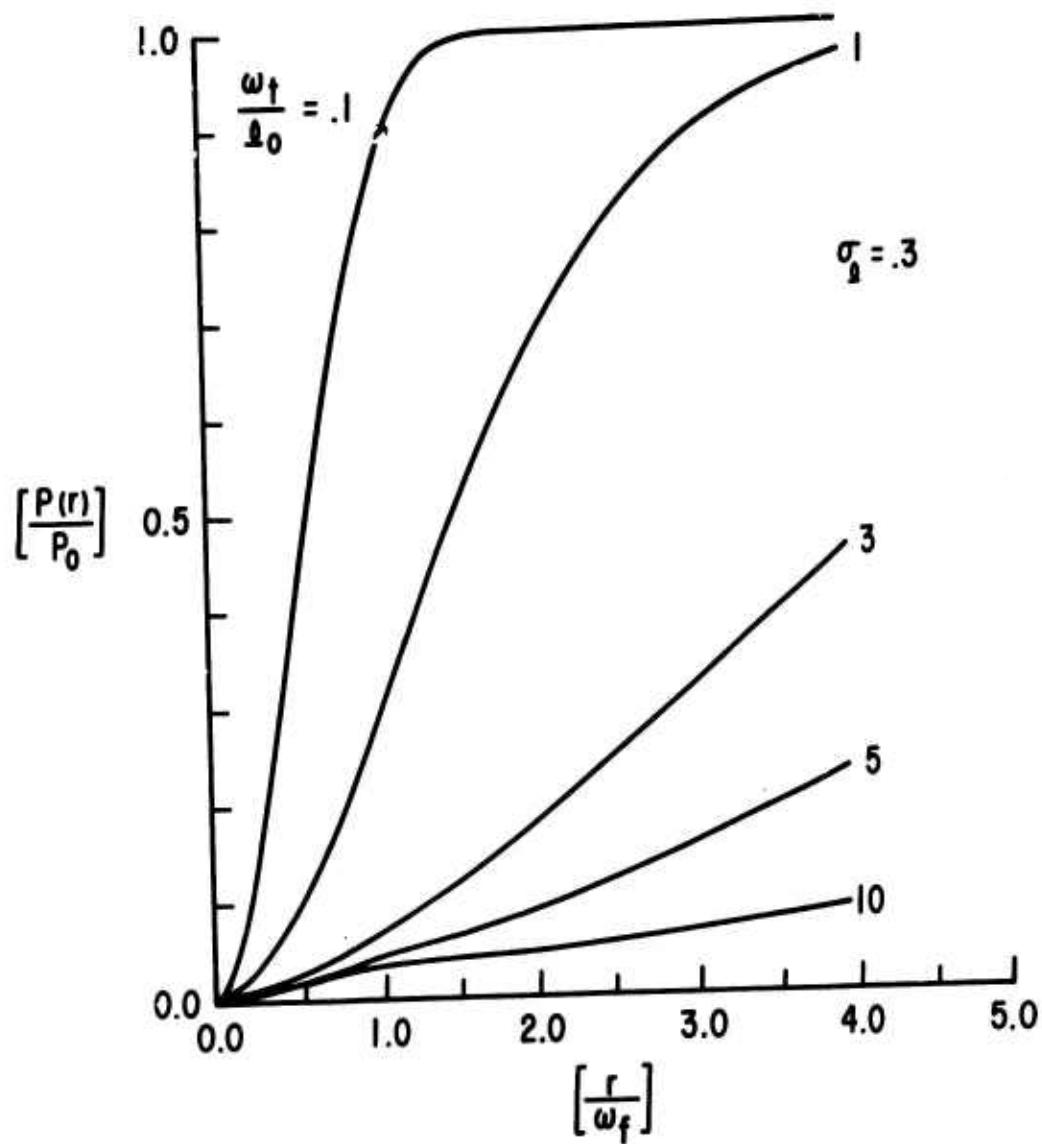
(a) $\sigma_l = 0.1$ wavelength

Figure 3. Integrated Relative Power Profiles for the Same Cases Shown in Figure 2



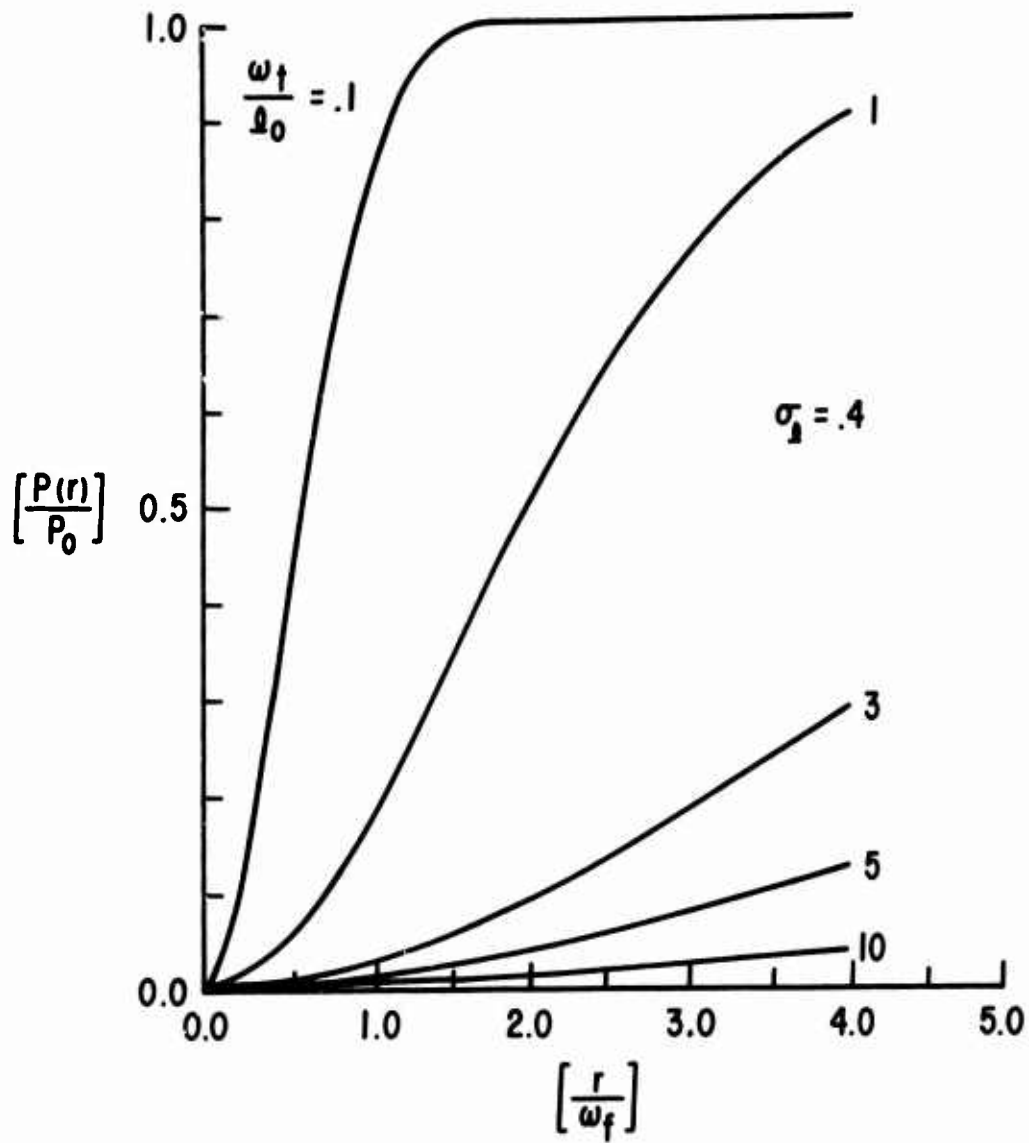
(b) $\sigma_\ell = 0.2$ wavelength

Figure 3. Integrated Relative Power Profiles for the Same Cases Shown in Figure 2



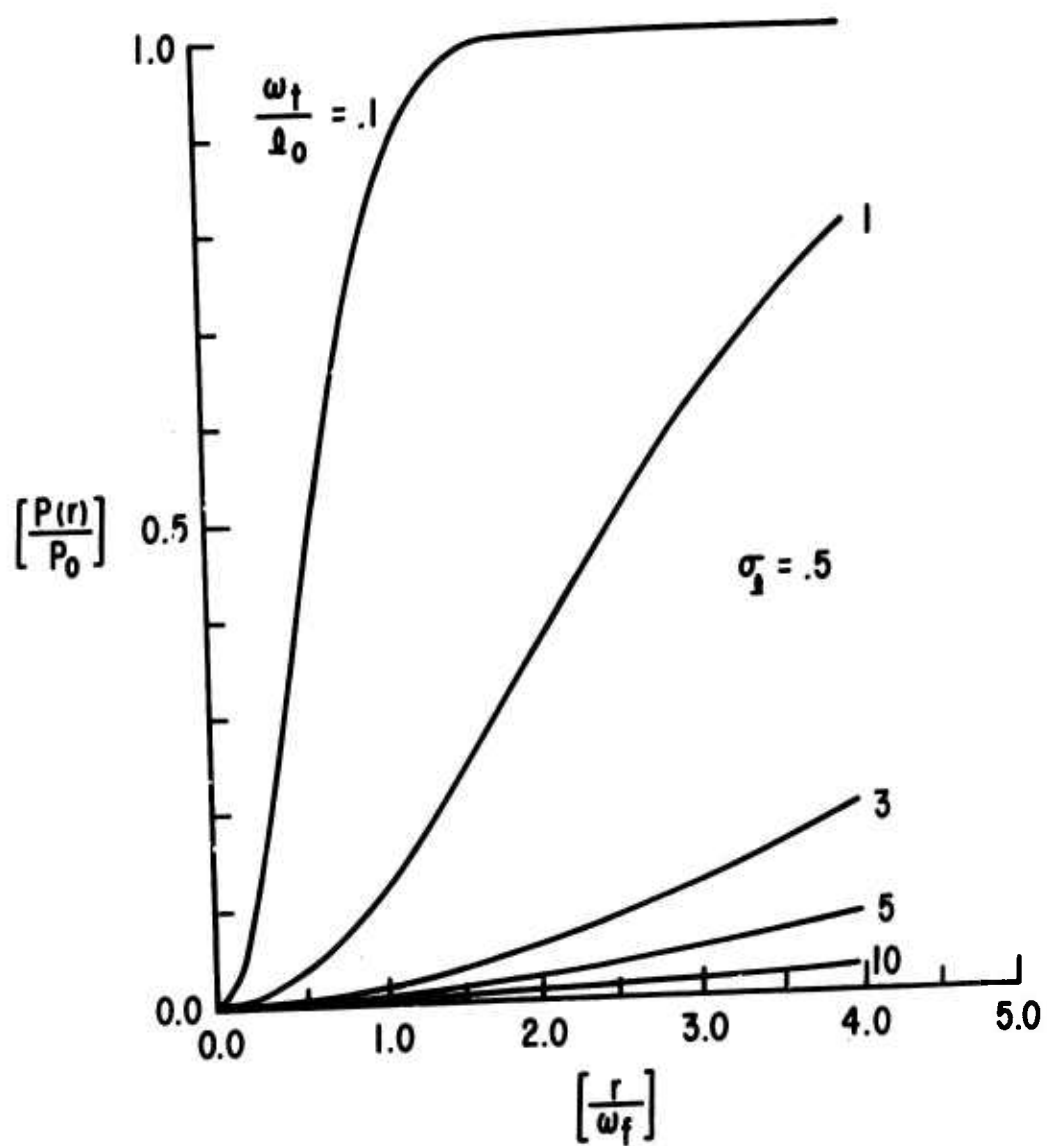
(c) $\sigma_l = 0.3$ wavelength

Figure 3. Integrated Relative Power Profiles for the Same Cases Shown in Figure 2



(d) $\sigma_l = 0.4$ wavelength

Figure 3. Integrated Relative Power Profiles for the Same Cases Shown in Figure 2



(e) $\sigma_l = 0.5$ wavelength

Figure 3. Integrated Relative Power Profiles for the Same Cases Shown in Figure 2

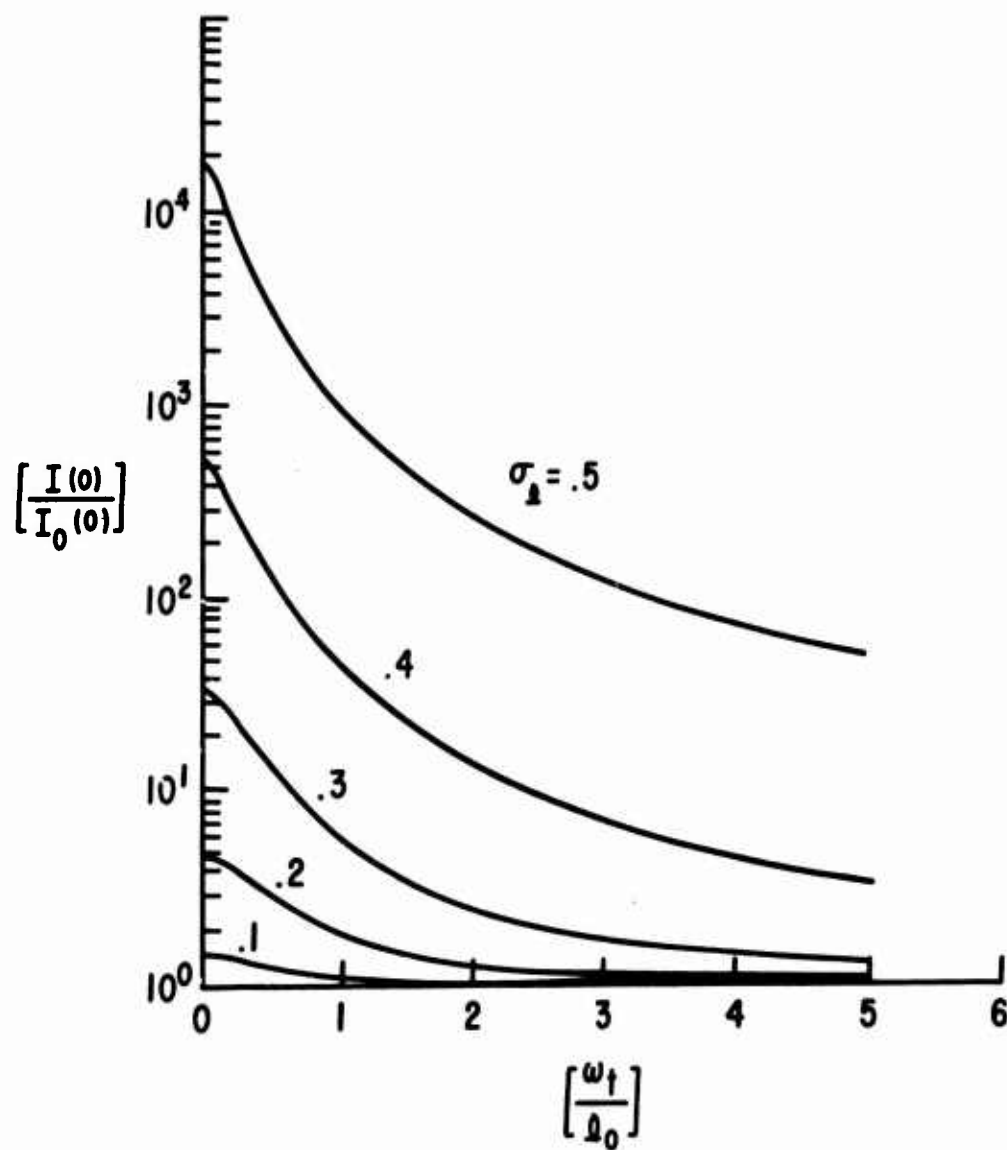


Figure 4. Relative Accuracy of the First Order Prediction for the Maximum Average Irradiance for Various Phase Distortions (σ_l) and Relative Phase Correlation Length (ω_t/l_0)

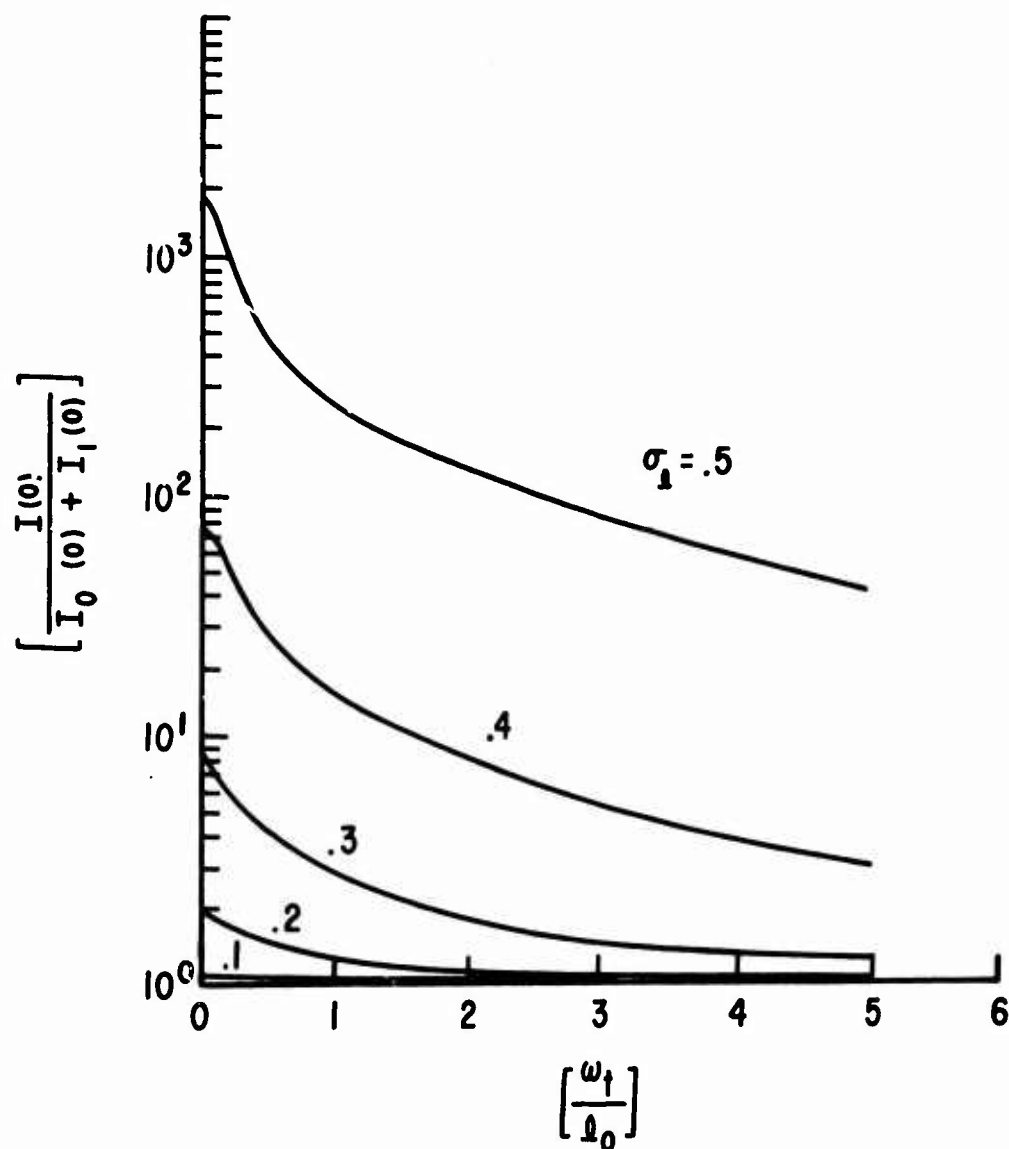


Figure 5. Relative Accuracy of the Second Order Prediction for the Maximum Average Irradiance for Various Phase Distortions (σ_1) and Relative Phase Correlation Length (ω_t / l_0)

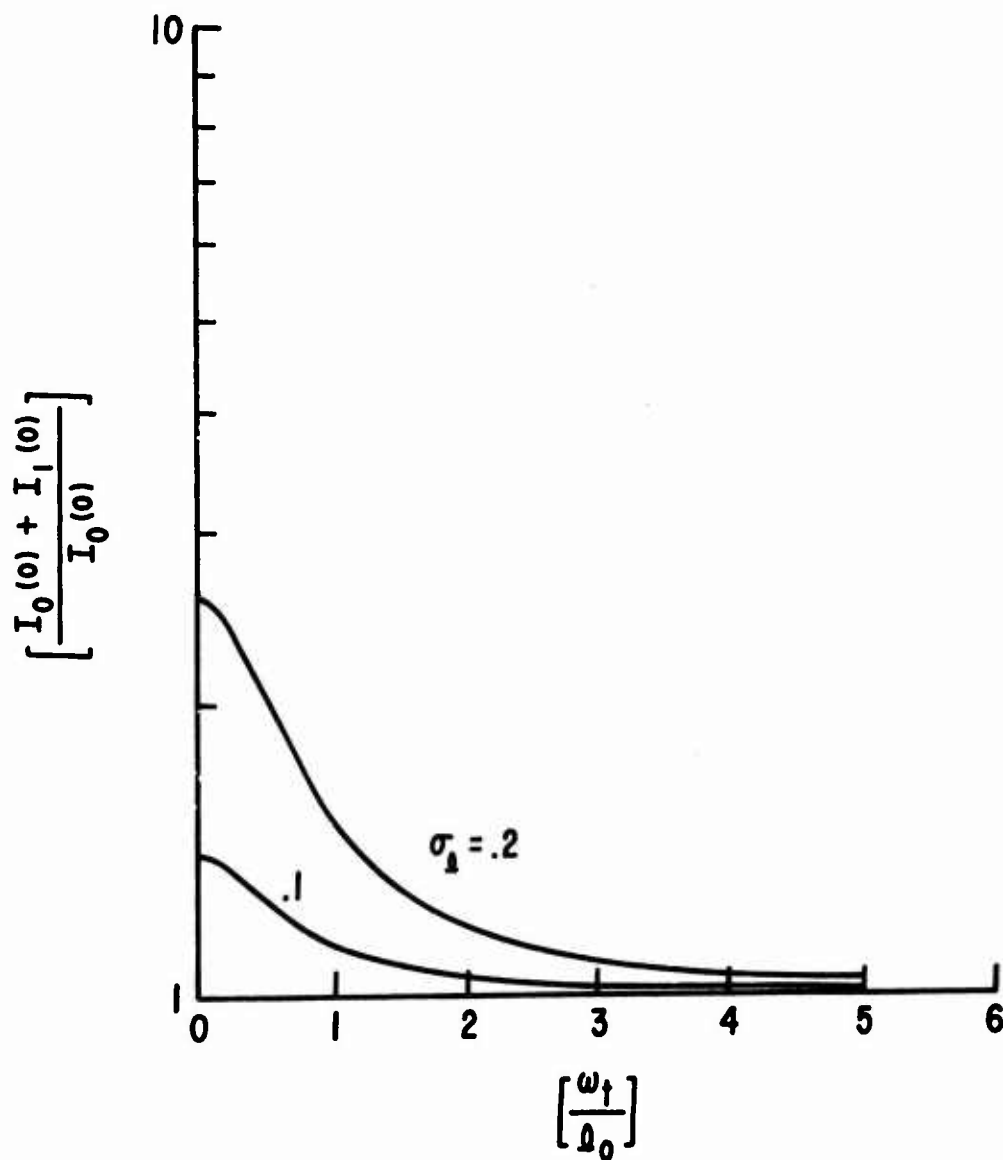
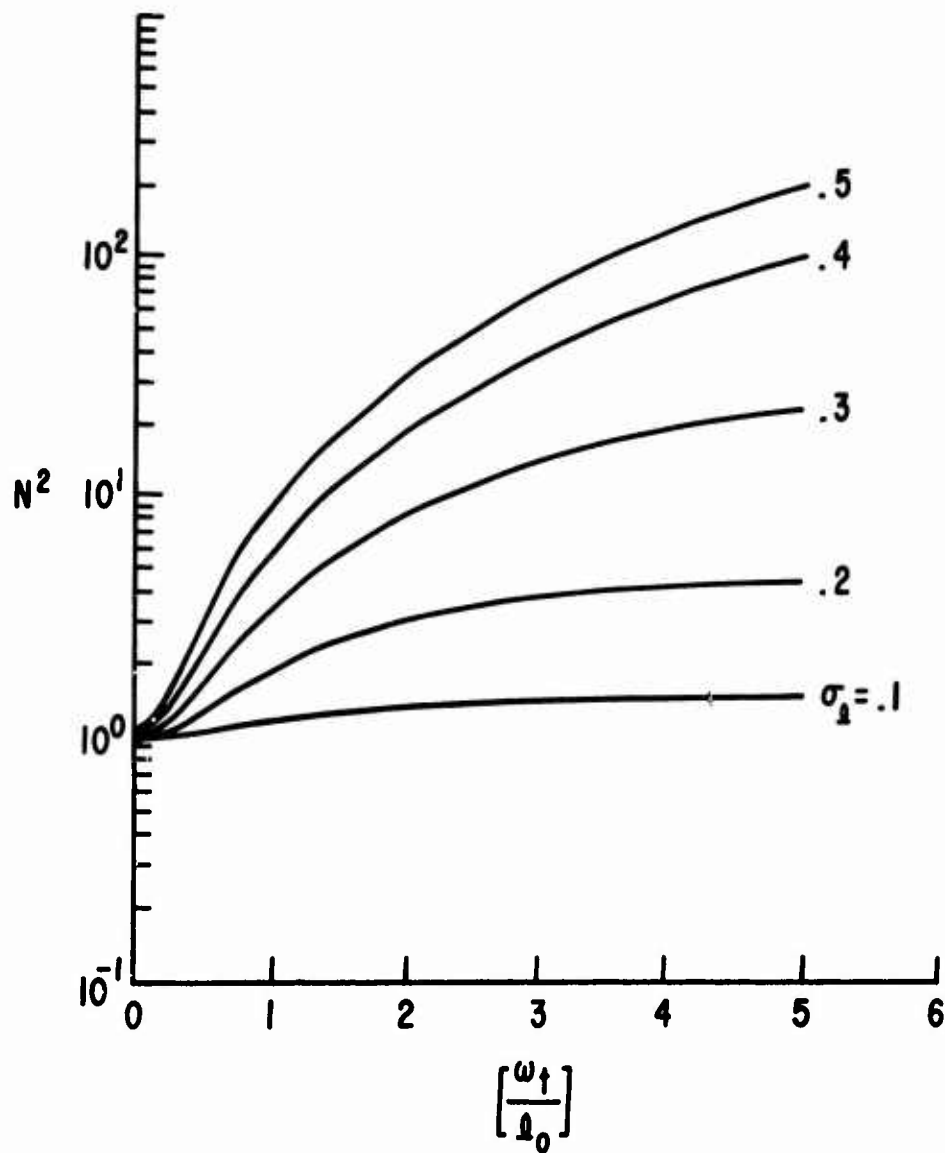
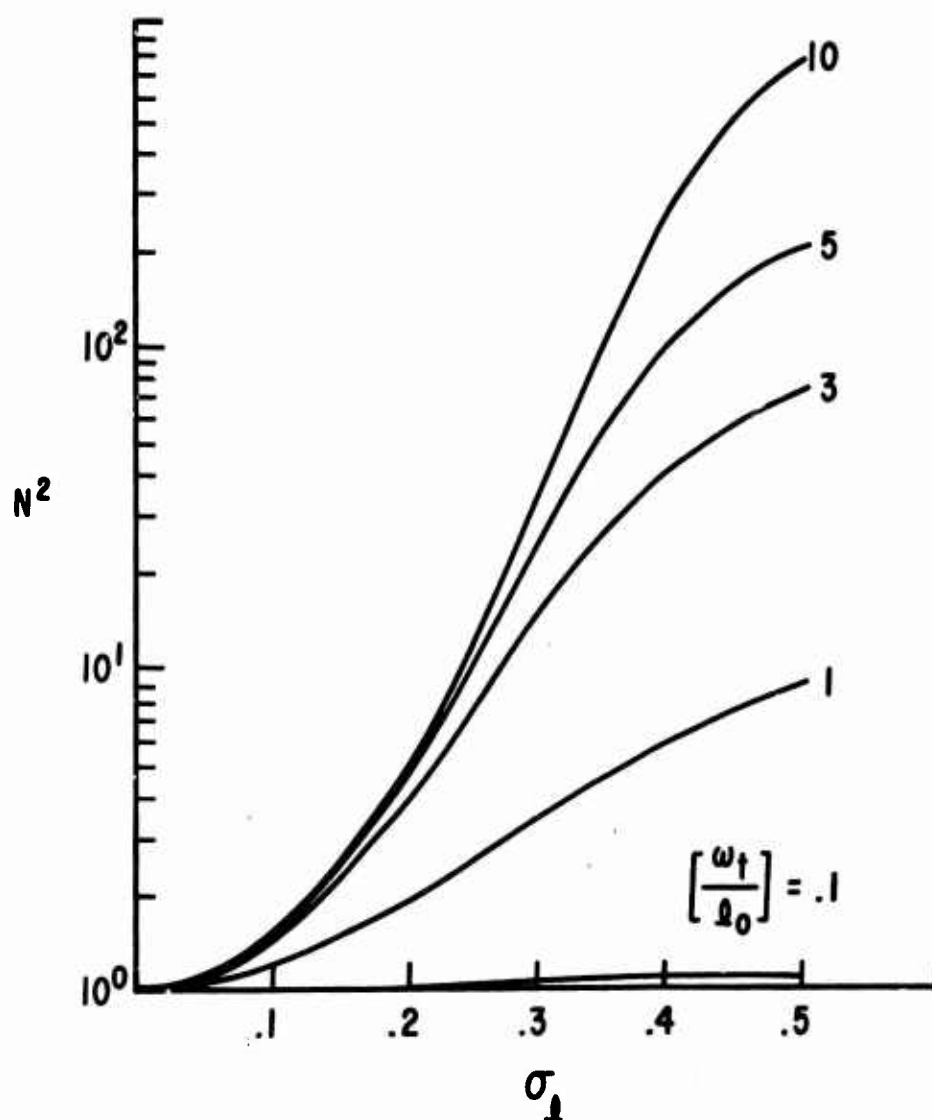


Figure 6. Ratio of Second Order to First Order Prediction for the Maximum Average Irradiance for $\sigma_0 = 0.1$ and 0.2 wavelength Versus the Relative Phase Correlation Length (ω_t/ω_0)



(a) N^2 versus (ω_t/l_0)

Figure 7. N is the Number of Times Diffraction Limited that the Focal Plane Irradiance Distribution Becomes When One Uses Power in a Fixed Bucket as the Definition



(b) N^2 versus (σ_l)

Figure 7. N is the Number of Times Diffraction Limited that the Focal Plane Irradiance Distribution Becomes When One uses Power in a Fixed Bucket as the Definition

It can be shown that the OTF for simple telescope jitter is

$$M_j(x,y) = \exp \left\{ - \frac{k^2 \overline{\theta^2}}{4} (x^2 + y^2) \right\} \quad (23)$$

where $\overline{\theta^2}$ is the 1-sigma line-of-sight, two-axis jitter variance. Comparing equations (22) and (23), the effect of the large scale phase aberrations is to provide a source of beam jitter. Then

$$\overline{\theta^2} = \frac{4(\sigma_\ell^2)(\lambda^2)}{\ell_0^2} \quad (24)$$

where equation (1) has been used. The strength of the effective jitter decreases with increasing correlation length and increases with the magnitude of the phase variance. A typical value for $\overline{\theta^2}$ can be obtained for $\sigma_\ell = 0.2$, $\lambda = 10.6 \mu\text{m}$, and $\ell_0 = 0.5\text{m}$ equal to

$$\sqrt{\overline{\theta^2}} \approx 7 \mu\text{rad}$$

The irradiance distribution takes the form

$$\langle I(r) \rangle = I_0 \left[\frac{1}{1 + \frac{k^2 \overline{\theta^2} \omega_t^2}{2}} \right] \cdot \exp \left[- \frac{2r^2}{\omega_f^2} \cdot \left(\frac{1}{1 + \frac{k^2 \overline{\theta^2} \omega_t^2}{2}} \right) \right] \quad (25)$$

or using the definitions of ω_f and I_0 , gives

$$\langle I_f(r) \rangle = I'_0 \exp \left[- \frac{2r^2}{(\omega'_f)^2} \right] \quad (26)$$

where

$$I'_0 = \frac{2P_0}{\pi(\omega'_f)^2} = I_0 \left(\frac{\omega_f}{\omega'_f} \right)^2 \quad (27)$$

$$(\omega_f')^2 = (\omega_f^2 + 2 f^2 \bar{\theta}^2) \quad (28)$$

As the relative size of the phase correlation length is decreased (R increasing), the focal plane irradiance distribution transitions from one dominated by narrow angle jitter, through intermediate stages, and finally to a distribution that is dominated by wide angle scattering. This is evidenced by the apparent leveling of the irradiance curves at large radial positions representing an almost constant background illumination that is characteristic of extremely wide angle scattering. The central portion of these curves is seen to have a shape that is much like a Gaussian curve; this result was discussed earlier in this report [equation (4)], as well as in reference 1. These curves represent the case where the beam is composed of two beams; one is simply an attenuated version of the original beam, while the second arises from a very widely scattered beam. In this situation the beam can be approximated well by

$$\langle I(r) \rangle = I_d(r) \exp(-\sigma_\phi^2) \quad (29)$$

The width of the beam (to the e^{-2} intensity level) is clearly just ω_f for this situation, and the relative maximum intensity reduction is $\exp(-\sigma_\phi^2)$, as compared to $(\omega_f^2/\omega_f^2 + 2 \bar{\theta}^2 f^2)$ for the preceding case.

These contrasting situations represent the two extremes obtained in the limit of very small and very large relative phase correlation lengths (ω_t/ℓ_0) , and clearly show the effect of phase correlation length on the far-field irradiance distribution.

For the largest values of $\sigma_\ell \geq 0.4$, the attenuation of the original beam is so severe $[I_d(r) \exp(-\sigma_\phi^2)]$ that all the energy appears in the second beam at very widely scattered angles. When the phase distortions become this strong, one can use an altered picture for the propagation process. Since $\exp[-\sigma_\phi^2 (1 - e^{-r^2/\ell_0^2})]$ will be very small for almost all values of $r > 0$ when σ_ϕ^2 is large, the exponential can be expanded and again equation (22) is obtained. In other words, all the energy scattered into the incoherent second beam can be visualized at a very large angular jitter source again given by equation (24). This is true except when the correlation length is much, much less than the aperture diameter. Letting $\sigma_\ell = 0.5$, $\ell_0 = 0.25$ m, and $\lambda = 10.6$ μ m, the result is

$$\sqrt{\theta^2} \approx 45 \text{ } \mu\text{rad}$$

For apertures on the order of this ℓ_0 and larger, the far-field angular spot size is on the order of 12 μ radians and smaller. Therefore, this effective jitter is very large, and acts to spread the beam to a size several times larger than its ideal diffraction limited size.

In figures 3(a) through (e), the irradiance curves have been integrated to give power versus bucket radius curves. The preceding comments regarding the irradiance curves are also appropriate to bucket radius curves. Of particular interest, note that for $\left(\frac{\omega_t}{\ell_0}\right) \geq 3$, the power contained in $\left(\frac{r}{\omega_f}\right) = 1$ is almost the same, indicating that for all these cases the central portion of the beam is approximately the same. Again this shows the applicability of the two beam model described in reference 1. It also shows that for a wide range of values of $\left(\frac{\omega_t}{\ell_0}\right)$ and σ_ℓ , equation (29) is a useful and accurate representation of the beam. Of course, for the larger values of σ_ℓ , this concept begins to fail, and its range of usefulness is best studied with the figures discussed in the following paragraphs.

In figure 4, the ratio of the on-axis intensity of equation (15) to the first term in the expansion, which is simply equation (3), is shown for different relative phase correlation lengths and strengths of phase distortion. When this ratio is close to unity, the approximation of equation (3) provides an accurate estimate of the maximum irradiance. Suppose a ratio of 1.5 is set as an acceptable upper bound to the required accuracy. Then, except for the case where $\sigma_\ell \approx 0.1$, smaller and smaller correlation lengths (for constant σ_ℓ) are required to satisfy this criterion. For example, with $\left(\frac{\omega_t}{\ell_0}\right) \geq 5$, the criterion is satisfied only when $\sigma_\ell < 0.3$.

Figure 5 is a plot of the ratio of the on-axis intensity of equation (15) to the sum of the first two terms in the expansion (equation 4) versus the relative size of the phase correlation length for different strengths of phase distortion. A comparison of these results with the results of figure 3 indicates the degree of improvement obtained for the prediction of the intensity when a first order correction is made to account for the effect of a finite correlation length. The most significant improvement occurs for $\left(\frac{\omega_t}{\ell_0}\right) < 1$, as might be expected. For instance, when $\sigma_\ell = 0.2$ and $\left(\frac{\omega_t}{\ell_0}\right) = 1$, the accuracy criteria are obtained (as defined previously) by the second order expansion,

while the simpler first order expansion fails to meet the error condition. Also, in this situation, the case of $\sigma_\ell = 0.3$ exceeds the accuracy criteria for $\left(\frac{\omega t}{x_0}\right) \geq 3$, as compared to $\left(\frac{\omega t}{x_0}\right) \geq 5$ for the first order expansion.

A more sensitive representation of the difference between the first order and second order approximation can be obtained if the simple ratio of these quantities is plotted as a function of relative phase correlation length. Figure 6 shows this result for $\sigma_\ell = 0.1$ and 0.2 . Clearly, while the difference is negligible for very small relative correlation lengths $\left(\frac{\omega t}{x_0} \geq 1\right)$, it can be substantial for the larger values of x_0 $\left(\frac{\omega t}{x_0} \leq 1\right)$. This implies that, in some instances, much can be gained by using the second order expansion of equation (4), rather than the simple first order expansion of equation (3). For $\sigma_\ell > 0.2$, the differences in the predicted irradiance values will be even greater, of course.

In figure 7(a), the power contained in a bucket of radius ω_f (normalized to the total power) is plotted as a function of the relative phase correlation length for different strengths of phase distortion. Figure 7(b) is a plot of the same data, simply reversing the dependence of the correlation length and strength of phase distortion. The ordinate of these graphs is labeled with N^2 , N representing the number of times that the focal plane spot size of the beam is diffraction limited. This is a frequently used definition of the non-diffraction limited nature of optical beams. A second definition frequently used specifies the ratio of the radius of a power bucket needed to collect a prespecified amount of the total transmitted energy to the bucket radius needed for the diffraction limited beam. While the definition for N^2 used in figure 7(a) shows some dependence on the relative size of the phase correlation length, this dependence becomes weaker with increasing $\left(\frac{\omega t}{x_0}\right)$. On the other hand, the second definition of N^2 just discussed would show (for $\sigma_\ell > 0.1$) a strong dependence on the relative phase correlation length. The definition used for figures 7(a) and 7(b) is usually a better description of beam quality of an optical system. Other considerations, such as the impact of beam shape on material effects enters into this conclusion as well. Finally, with this definition of N^2 , a strong dependence on σ_ℓ is observed, as shown in figure 7(b). Hence, σ_ℓ should be as small as possible in any practical system design.

SECTION III

SOME OBSERVATIONS APPROPRIATE TO THE RANDOM PHASE SCATTERING PROCESS

Additional insight can be gained about the nature of the random phase scattering process by first using a generalization of the results of equation (13)

$$\langle I(x_0, y_0) \rangle = \int_{-\infty}^{\infty} \int_{-\infty}^{\infty} M_d(x, y) \cdot M_p(x, y) \cdot e^{-\left[i \frac{k}{f} (xx_0 + yy_0) \right]} dx dy \quad (30)$$

and then noting that

$$I_d(x_0, y_0) = \int_{-\infty}^{\infty} M_d(x, y) \cdot e^{-\left[i \frac{k}{f} (xx_0 + yy_0) \right]} dx dy \quad (31)$$

The following equation can then be written

$$M_d(x, y) = \left(\frac{k}{2\pi f} \right)^2 \int_{-\infty}^{\infty} I_d(x_0, y_0) e^{+\left[i \frac{k}{f} (xx_0 + yy_0) \right]} dx_0 dy_0 \quad (32)$$

which, when substituted into equation (29), results in

$$\langle I(x_0, y_0) \rangle = \int_{-\infty}^{\infty} I_d(x, y) Q(x_0 - x, y_0 - y) dx dy \quad (33)$$

where

$$Q(x, y) = \left(\frac{k}{2\pi f} \right)^2 \int_{-\infty}^{\infty} M_p(x_0, y_0) e^{-\left[i \frac{k}{f} (x_0 x + y_0 y) \right]} dx_0 dy_0 \quad (34)$$

The result is that the focal plane irradiance distribution is the convolution of the ideal diffraction limited irradiance distribution with the function $Q(x, y)$. This latter function is the Fourier transform of the random phase aberration OTF.

In the limit of very small aberrations, $\sigma_\ell \rightarrow 0$ and also $M_p(r)$ approaches a constant value of unity. For that case, $Q(x,y)$ is a delta function at $x=y=0$, with the obvious result that $\langle I(x_0, y_0) \rangle = I_d(x_0, y_0)$.

For non-zero random phase aberrations, the OTF can be written as shown in equation (8). A typical form for this equation is shown in figure 8. The asymptotic limit of $M_p(r)$, for large r , is $\exp(-\sigma_\phi^2)$. Consider writing $M_p(r)$ as

$$M_p(r) = \exp(-\sigma_\phi^2) + (1 - \exp(-\sigma_\phi^2)) f(r) \quad (35)$$

where $f(r)$ is a function that approaches zero for large r . The shape of $f(r)$ resembles the OTF for simple jitter which was seen in equation (23) to be Gaussian. Taking the transform of $M_p(r)$ in equation (34) the following result is obtained

$$Q(x,y) = \exp(-\sigma_\phi^2) \delta(x,y) + (1 - \exp(-\sigma_\phi^2)) F(f(r)) \quad (36)$$

where $F(\cdot)$ denotes the Fourier transformation and where $\delta(x,y)$ is the Dirac delta function. Conceptually, it is useful to consider the two functions of equation (35) as synthetic apertures superimposed on the original telescope aperture function. As such, the first function, $\exp(-\sigma_\phi^2)$, clearly has no radial limiting effect, and is simply a source of power attenuation. Its Fourier transform is a delta function and thus does not change the spatial characteristics of $I_d(r)$ when the convolution in equation (33) is performed. The second function is the product of a simple energy extinction term

$1 - \exp(-\sigma_\phi^2)$ with a "bell-shaped" function that asymptotically approaches zero as $r \rightarrow \infty$. A synthetic aperture function of this type will produce a transformed function whose width is inversely proportional to its initial width, and whose central amplitude is proportional to the area of $f(r)$. For instance, if the synthetic aperture function is very narrow compared to the effective physical aperture of the output beam, then the projection of $f(r)$ in the focal plane of the optical system [i.e., the Fourier transform of $f(r)$] will be very wide compared to the width of the ideal diffraction limited pattern, $I_d(r)$. This will usually be the case when the correlation length of the phase fluctuations are smaller than the output aperture dimension. Convolving these two functions with each other will produce a beam that is spread more than either

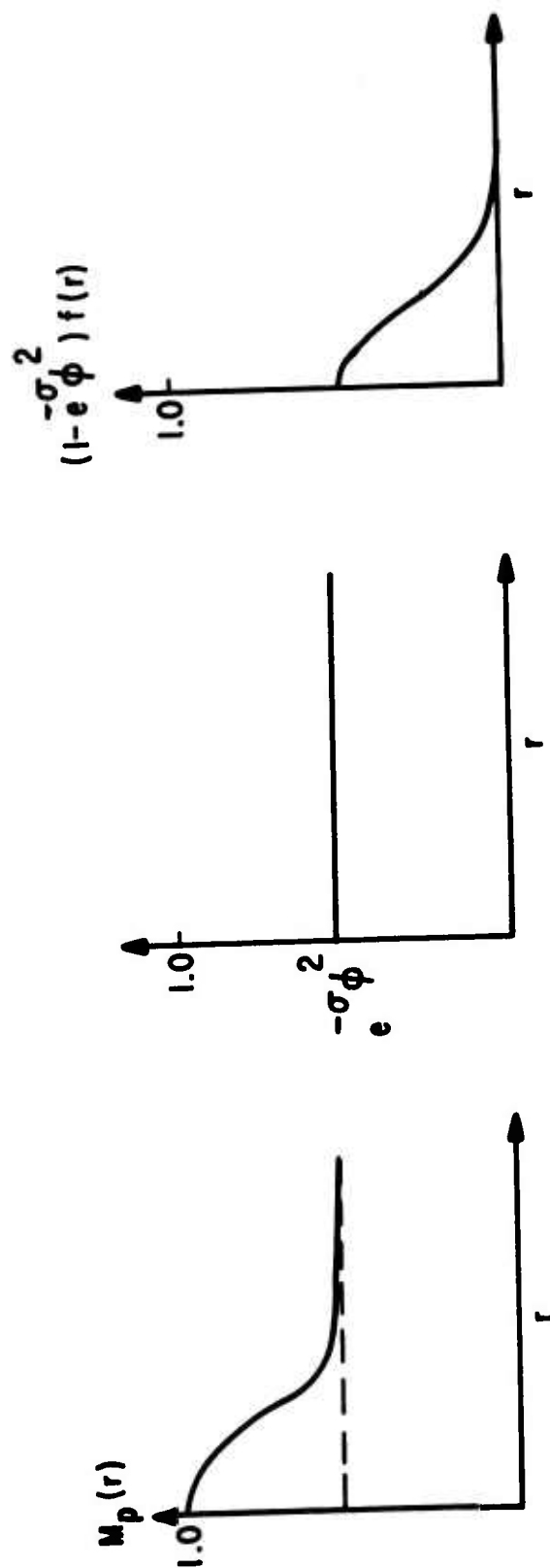


Figure 8. Typical Modulation Transfer Function for a Random Phase Distortion Decomposed into Two Separate Functions

$F(f(r))$ or $I_d(r)$.

On the other hand, if $f(r)$ is wide compared to the laser beam output aperture size, then its projection in the focal plane will be smaller than $I_d(r)$. If $f(r)$ is sufficiently broad, or in other words, if the phase fluctuations are highly correlated over dimensions the size of the output aperture, then the Fourier transformed function will be so narrow that when it is convolved with $I_d(r)$ in equation (33), it will act very much like a delta function. Only slight spreading of the original diffraction limited function will occur.

The width of $f(r)$ is thus very important in describing exactly how the second term in equation (36) will affect the spreading of $I_d(r)$ by the convolution in equation (33). While to some extent, the width must be closely related to the correlation length of the phase fluctuations, it is also a function of the variance of the fluctuations.

1. EXACT SOLUTION

If the random phase OTF is expanded in the same manner as in section II and assumes a Gaussian covariance function, such as equation (10), then the following result is obtained for equation (33):

$$\langle I(x,y) \rangle = \sum_{n=0}^{\infty} \frac{\sigma_{\phi}^{2n} \exp(-\sigma_{\phi}^2)}{n!} \cdot [I_d(x,y) * I_n(x,y)] \quad (37)$$

where "*" means convolution, and where

$$I_n(r) = \frac{2}{\pi \omega_n^2} \cdot \exp\left(-\frac{2r^2}{\omega_n^2}\right) \quad (38)$$

$$\omega_n^2 = 2n \left(\frac{2f}{k \ell_o} \right)^2 \quad (39)$$

Note that $I_0(r) = \delta(x,y)$ in equation (38). Each term in the series solution is the convolution of $I_d(r)$ with a Gaussian function. Because the Fourier transform of a Gaussian function is itself Gaussian in shape, equation (23) can be inserted into equation (34), and also each term in equation (37) represents the convolution of the diffraction limited focal plane distribution with a source of angular jitter given by

$$\overline{\theta_n^2} = \frac{4n}{k^2 \ell_0^2} \quad (40)$$

If it is assumed that

$$I_d(r) = I_0 e^{-(2r^2/\omega_f^2)}$$

and

$$\omega_f^2 = \left(\frac{2f}{k\omega_t} \right)^2$$

then the operations specified by equation (37) will produce an infinite series of Gaussian functions, each successive function having a transverse size larger than any of the preceding functions. The focal plane distribution is thus built up as the sum of independent Gaussian beams, all of whose respective spot sizes are larger than the original beam size of ω_f . This result was earlier seen in equation (15).

Writing equation (37) as

$$\exp(-\sigma_\phi^2) I_d(x,y) + \sum_{n=1}^{\infty} \frac{\exp(-\sigma_\phi^2) \sigma_\phi^{2n}}{n!} \left[I_d(x,y) * I_n(x,y) \right]$$

the second term clearly describes the effect that the function $f(r)$ of equation (35) has on the convolution of equation (33). For this approach then a picture is obtained that describes this part of the scattering process as a complicated multi-jitter type convolution. But by equation (38), the respective jitter components are characterized only by the random phase correlation length, with no dependence on the phase variance.

2. SIMPLIFIED QUANTITATIVE RESULTS FOR STRONGLY PHASE ABERRATED NONDIFFRACTION LIMITED BEAMS

While the results developed thus far for the description of the far-field irradiance distribution of a random phase aberrated optical system are exact within the limitations of the assumptions and approximations made here, they do not provide particularly useful insight into the dependence of the important

characteristics of the beam on the phase variance σ_ϕ^2 and the phase correlation length. This is true even if a few of the higher order terms are kept in equation (15), although an improved estimate of the far-field irradiance characteristics does result by this procedure (figures 4, 5 and 6).

The scattering process can be visualized better by taking the approach that the function $f(r)$ in equation (35) can be approximated by a Gaussian function of unit amplitude and some characteristic width. Recalling that the OTF for a system jitter source is Gaussian also, this approach is tantamount to treating all the scattered energy as a random tilting, or jittering of the beam. The total process then has the following interpretation. First, a certain fraction of the total beam energy is propagated completely unaffected by the phase distortions. This fraction of the total energy is given by $\exp(-\sigma_\phi^2)$ (equation 36). The remaining fraction of the energy that is scattered $(1 - \exp(-\sigma_\phi^2))$, is smeared or spread by a simple random jittering process. The angular spread associated with the jitter is related to the effective width of $f(r)$ as defined by L . Then, by writing

$$f(r) \approx \exp \left(-\frac{r^2}{L^2} \right) \quad (41)$$

and recalling the form of the OTF for pure telescope jitter (equation 23), the result is

$$\overline{\theta^2} = \left(\frac{2}{kL} \right)^2 \quad (42)$$

As the width of $f(r)$ increases (increasing L), the angular spread due to this synthetic jitter source decreases. Therefore a process that produces a large effective width of $f(r)$ will only slightly spread the remaining $(1 - \exp(-\sigma_\phi^2))$ fraction of the energy.

Clearly the width of $f(r)$ can be defined in many ways. One possible definition of an integral scale size was given in equation (11). That definition will be used here. Using equations (8) and (34), gives

$$f(r) = \frac{\exp(-\sigma_\phi^2)}{1 - \exp(-\sigma_\phi^2)} \exp \left(C_\phi(r) - 1 \right) \quad (43)$$

Assuming a Gaussian covariance function of the form $\left[\sigma_{\phi}^2 e^{-r^2/\ell_0^2} \right]$, the integral scale size is computed to be

$$L_0 = \frac{\exp(-\sigma_{\phi}^2)}{1-\exp(-\sigma_{\phi}^2)} \cdot \frac{\sqrt{\pi}}{2} \cdot \ell_0 \sum_{n=1}^{\infty} \frac{\sigma_{\phi}^{2n}}{n! \sqrt{n}} \quad (44)$$

where the exponential has been expanded in equation (43). Assuming the form of equation (41) for $f(r)$ results in

$$L = \frac{\exp(-\sigma_{\phi}^2)}{1-\exp(-\sigma_{\phi}^2)} \cdot \ell_0 \sum_{n=1}^{\infty} \frac{\sigma_{\phi}^{2n}}{n! \sqrt{n}} \quad (45)$$

Consider the form of L for small phase distortions, then

$$L \approx \ell_0 (1 - \sigma_{\phi}^2) \quad (46-a)$$

This limiting form shows that the width of $f(r)$ is directly proportional to the phase correlation length but that with increasing phase variance L decreases. A slightly more accurate form may be obtained by not expanding $\exp(-\sigma_{\phi}^2)$. One gets

$$L_1 = \left(\frac{\exp(-\sigma_{\phi}^2)}{1-\exp(-\sigma_{\phi}^2)} \right) \ell_0 \sigma_{\phi}^2 \quad (46-b)$$

Keeping second and third order terms in the series expansion, gives

$$L_2 = \left(\frac{\exp(-\sigma_{\phi}^2)}{1-\exp(-\sigma_{\phi}^2)} \right) \cdot \ell_0 \left(\sigma_{\phi}^2 + \frac{\sigma_{\phi}^4}{2\sqrt{2}} \right) \quad (47)$$

$$L_3 = \left(\frac{\exp(-\sigma_{\phi}^2)}{1-\exp(-\sigma_{\phi}^2)} \right) \cdot \ell_0 \cdot \left(\sigma_{\phi}^2 + \frac{\sigma_{\phi}^4}{2\sqrt{2}} + \frac{\sigma_{\phi}^6}{6\sqrt{3}} \right) \quad (48)$$

From equations (45) and (46), it is clear that L is always less than ℓ_0 for any

non-zero phase variance. However, for a fixed ℓ_0 and σ_ϕ^2 , the successive approximations to $L(L_1, L_2, L_3, \text{etc.})$ monotonically increase. Therefore the use of one of these values for L will make the angular spread of this energy larger than it actually is (equation 42), yielding a conservative (low) estimate for the maximum irradiance of the beam.

If the diffraction limited irradiance distribution is again assumed to be Gaussian, the scattered energy will also have a Gaussian form.

$$I_s(r) = [1 - \exp(-\sigma_\phi^2)] \cdot I_0 \left(\frac{\omega_f^2}{\omega_f^2 + 2 \overline{\theta^2} f^2} \right) \cdot \exp \left(-\frac{2r^2}{\omega_f^2 + 2 \overline{\theta^2} f^2} \right) \quad (49)$$

$\overline{\theta^2}$ is defined in equation (42). The unscattered energy will have the form

$$I_u(r) = \exp(-\sigma_\phi^2) \cdot I_0 \exp \left(\frac{2r^2}{\omega_f^2} \right) \quad (50)$$

An example of a typical far-field pattern is shown in figure 9. This result describes the far-field irradiance pattern as the sum of two Gaussian beams of different relative amplitudes and widths. Though simple in form, this approximation physically describes the salient features of the scattering process. For instance, if the phase variance is small ($\sigma_\phi \leq 0.1$) and the phase correlation length is much less than ω_1 , so that

$$L \approx \ell_0 \ll \omega_1 \quad (51)$$

then $I_s(r) \ll I_u(r)$ for all values of r , and the resulting irradiance distribution will be the same as the diffraction limited distribution multiplied by a scale factor $\exp(-\sigma_\phi^2)$. This is precisely the situation described by equation (3).

On the other hand, if σ_ϕ is large, so that $\exp(-\sigma_\phi^2) \ll 1$, then $I_u(r)$ is very small and may be negligible compared to $I_s(r)$, if L is not too small. If $\ell_0 \gg \omega_1$, then at least for some range of values of σ_ϕ^2 , L will be greater than ω_t . Physically, the scattering process should resemble a general smearing of the beam. This is exactly the result that equation (49) predicts.

Thus, this formulation provides a lucid picture of the nature of the

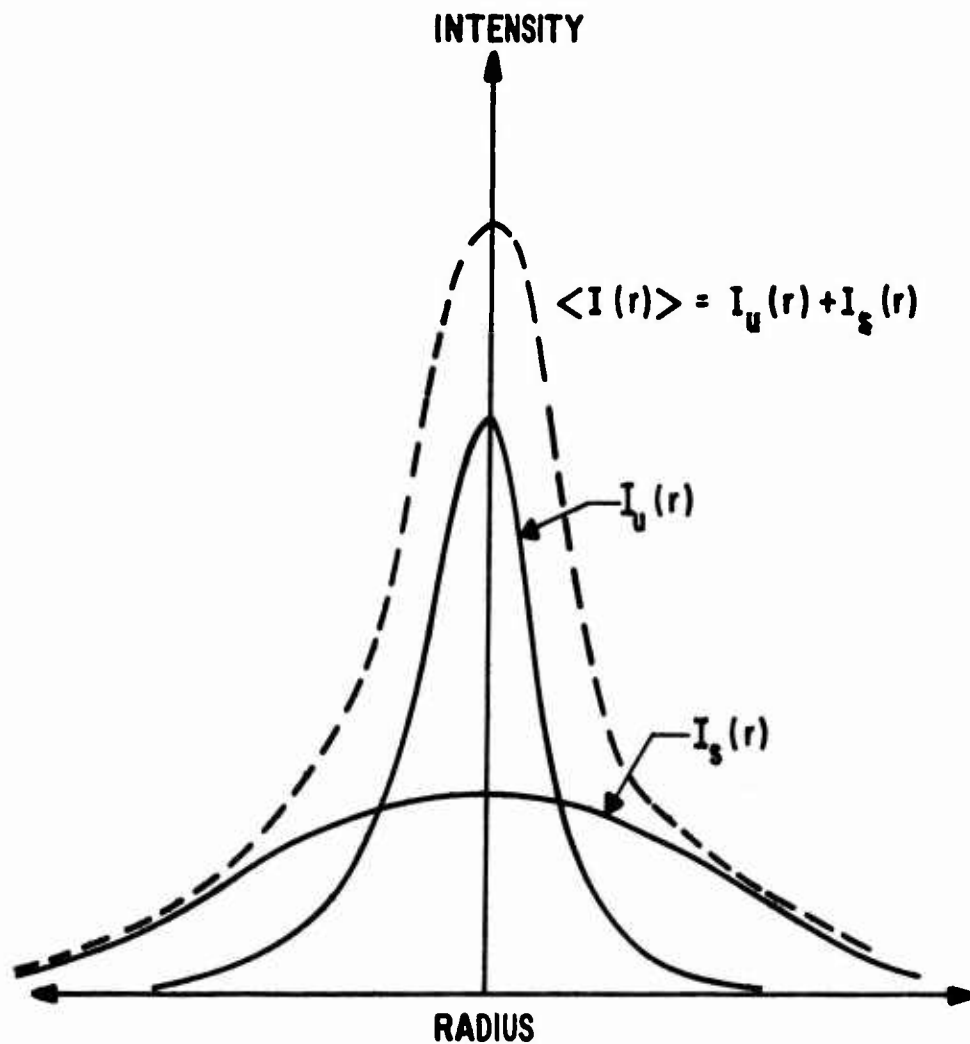


Figure 9. Typical Far-Field Irradiance Profile of a Phase Aberrated Nondiffraction Limited Beam Composed of the Sum of $I_u(r)$ and $I_s(r)$

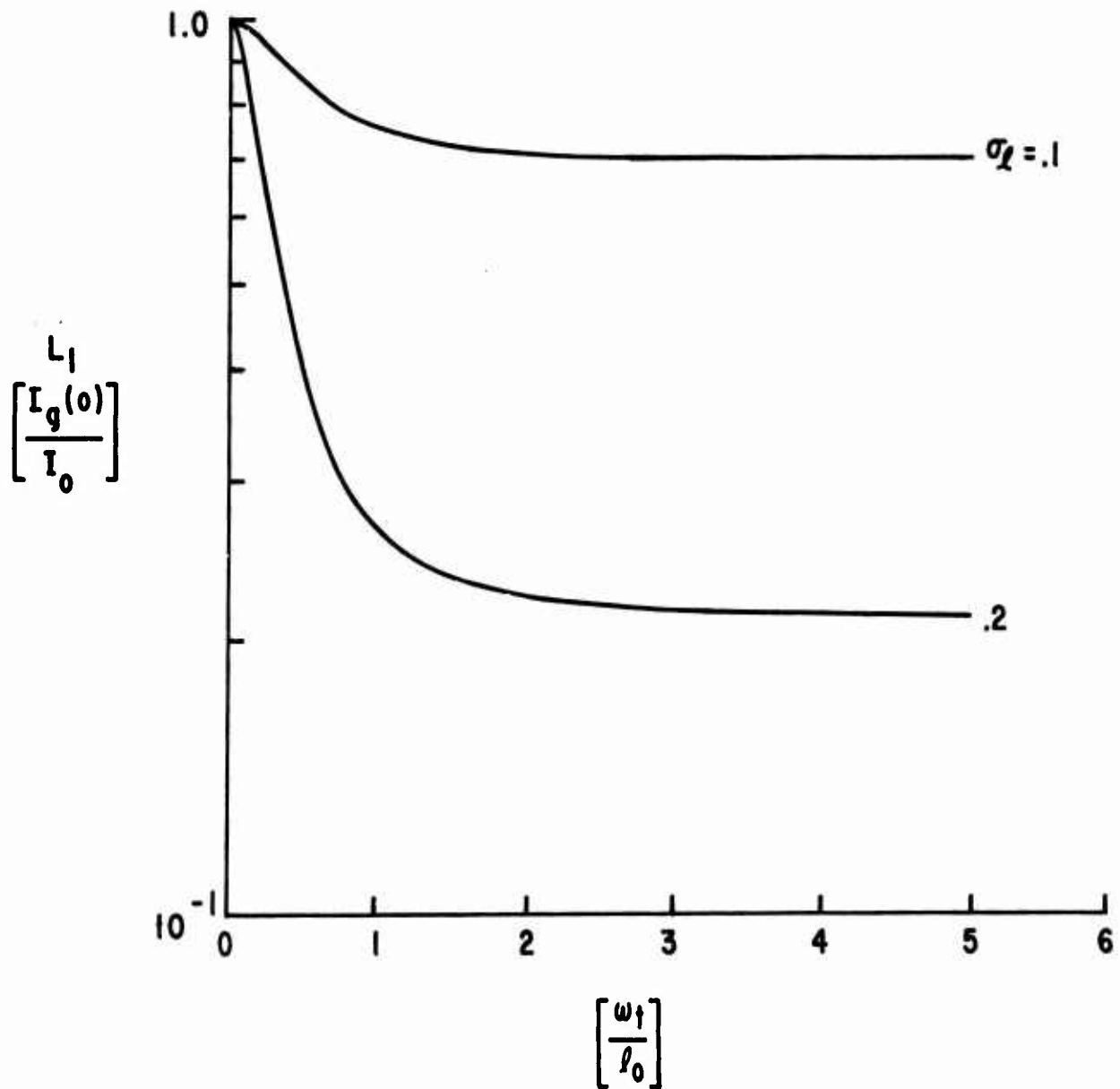
scattering process as a function of the important parameters. In addition, one of the approximations for L (equations 6 to 48) can be used to obtain an estimate of the focal plane irradiance distribution. While a few terms in the exact solution (equation 15) could also be used to estimate the focal plane distribution, the representation soon becomes cumbersome; furthermore, every one of these approximations fails to conserve the total energy in the beam.

The results obtained when the approximations to L are used can be seen in figures 10(a) through (c), where the on-axis intensity is plotted versus $\left(\frac{\omega t}{x_0}\right)$ for different phase variances. In figure 11 the same data are plotted, when L is computed from equation (45). Clearly, for small variances, the various approximations to L yield reasonably good estimates. However, it is also clear that for the larger of the variances, more terms are needed in the approximation to L .

Of course, these observations are of little consequence if this approximate method does not agree well with the exact analysis of section II. The agreement of the two methods can be judged by comparing the curves of figure 11 to those of figure 1, where the same data has been plotted for the exact solution. Plotting the ratio of these curves in figure 12, then over the range of the parameters studies, $0 \leq \sigma_\ell \leq 0.5$, and $0 \leq \frac{\omega t}{x_0} \leq 5$, the two results differ almost by 5 percent. The conclusion is that the fraction $f(r)$ (equation 43) can be represented very well by a single Gaussian function of the form of equation (41) where L is defined by equation (45).

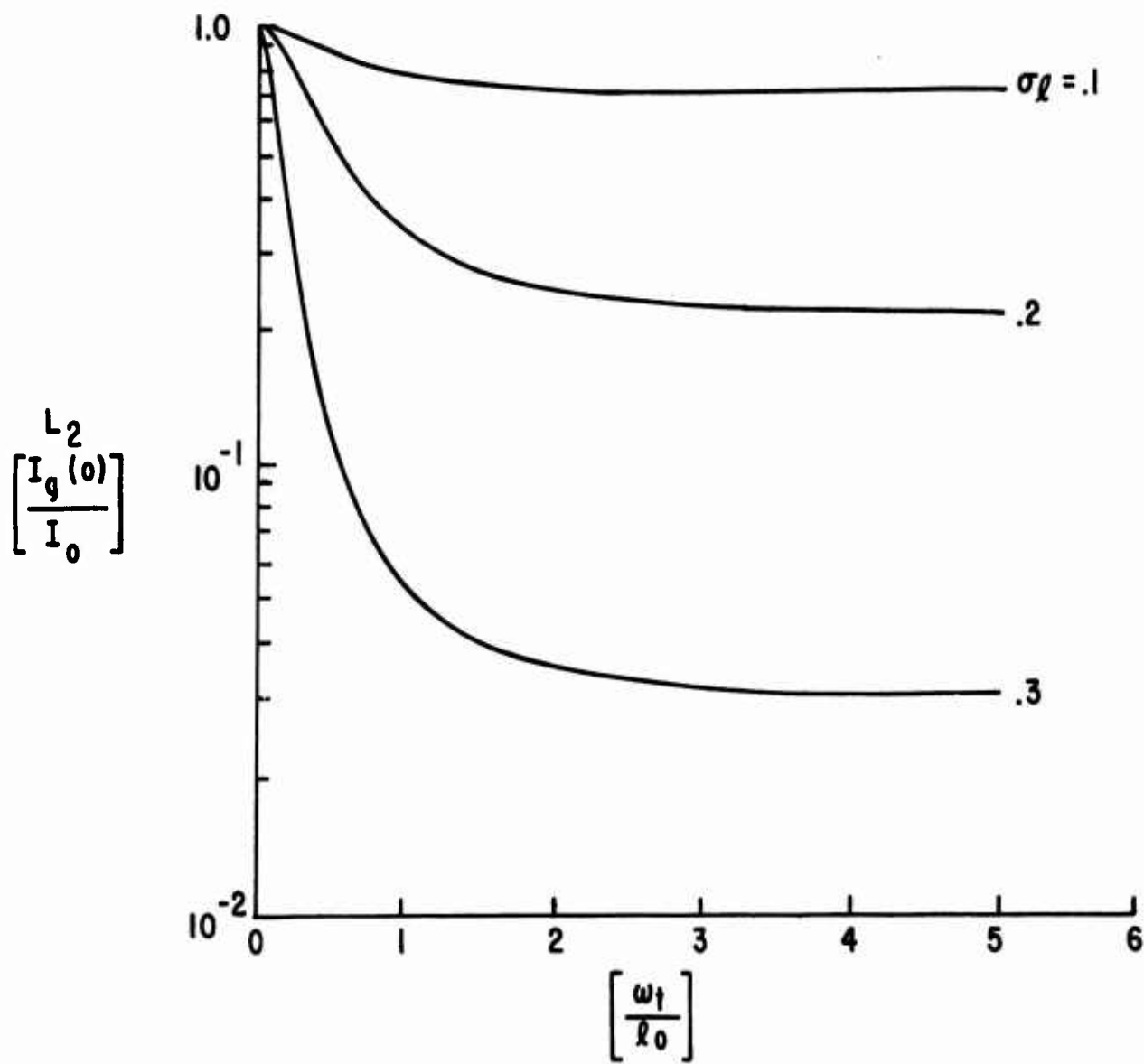
In addition, because L is a smoothly varying function of x_0 and σ_ℓ (see figure 13), one can very easily calculate the effect of phase aberrations on a Gaussian beam. This was done in equations (49) and (50). The peak amplitudes and relative shapes (e.g., figure 9) can easily be calculated once the effective correlation length L has been determined.

By contrast, to obtain similar information from the exact analysis of equation (15), the entire series must be completely summed for each value of r , σ_0 , and x_0 . Virtually no intuitive information about the nature and shape of the far-field irradiance distribution can be gained beforehand. Therefore, one of the major conclusions of this report is that the model developed by representing $f(r)$ in equation (43) by a Gaussian function is an accurate way of determining the characteristics of nondiffraction limited beams and in addition has an enhanced utility because of the ease with which important quantities can be estimated with a minimum of computational effort.



(a) L_1 scale approximation

Figure 10. Reduction in Relative Maximum Average Irradiance Using the Modified Two Gaussian Beam Model with the Different Approximations for the Scale Size L for Different rms Phase Distortions and Relative Correlation Lengths (ω_t/l_0)



(b) L_2 scale approximation

Figure 10. Reduction in Relative Maximum Average Irradiance Using the Modified Two Gaussian Beam Model with the Different Approximations for the Scale Size L for Different rms Phase Distortions and Relative Correlation Lengths (ω_t/ℓ_0)

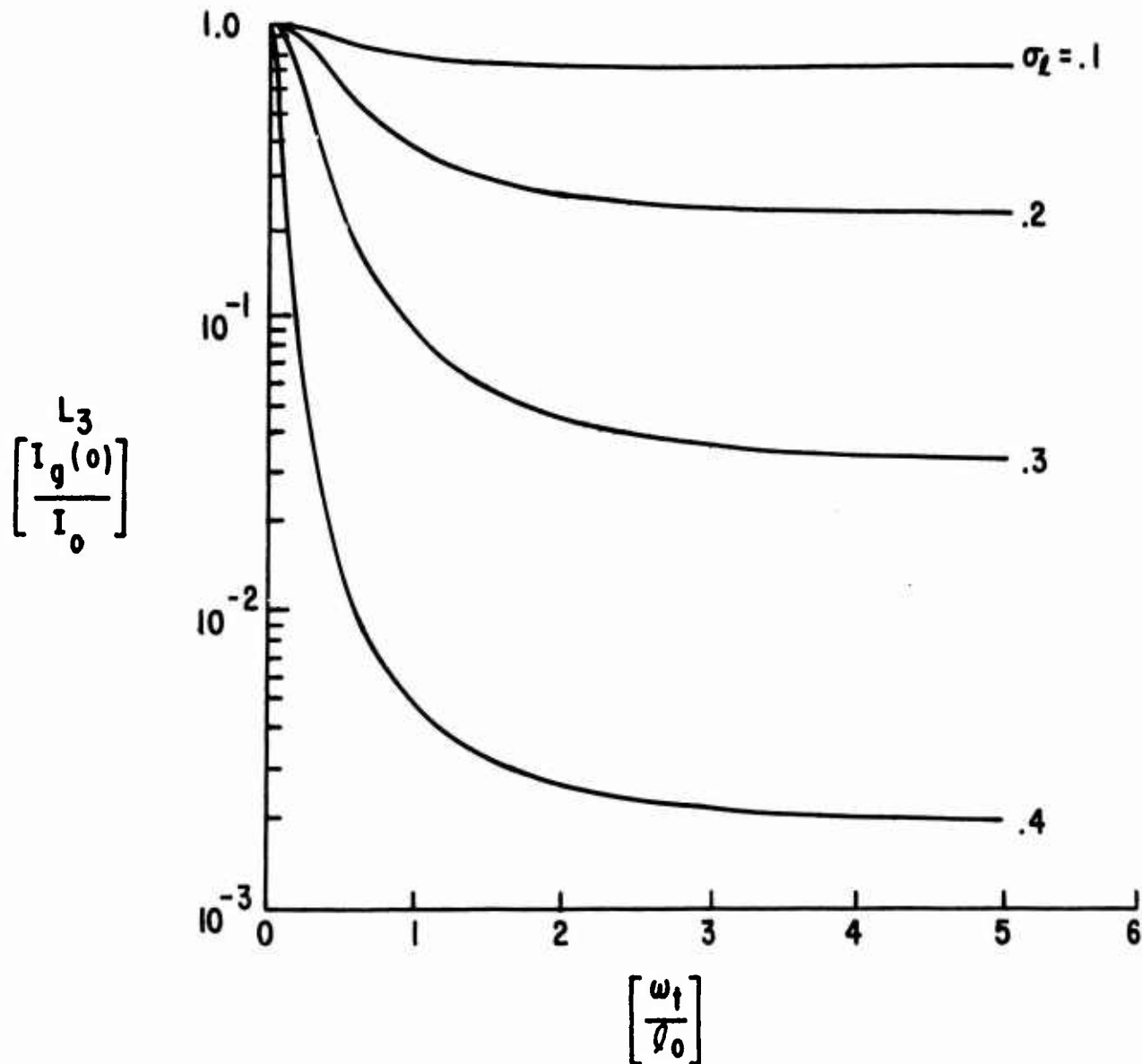
(c) L_3 scale approximation

Figure 10. Reduction in Relative Maximum Average Irradiance Using the Modified Two Gaussian Beam Model with the Different Approximations for the Scale Size L for Different rms Phase Distortions and Relative Correlation Lengths (ω_t/ℓ_0)

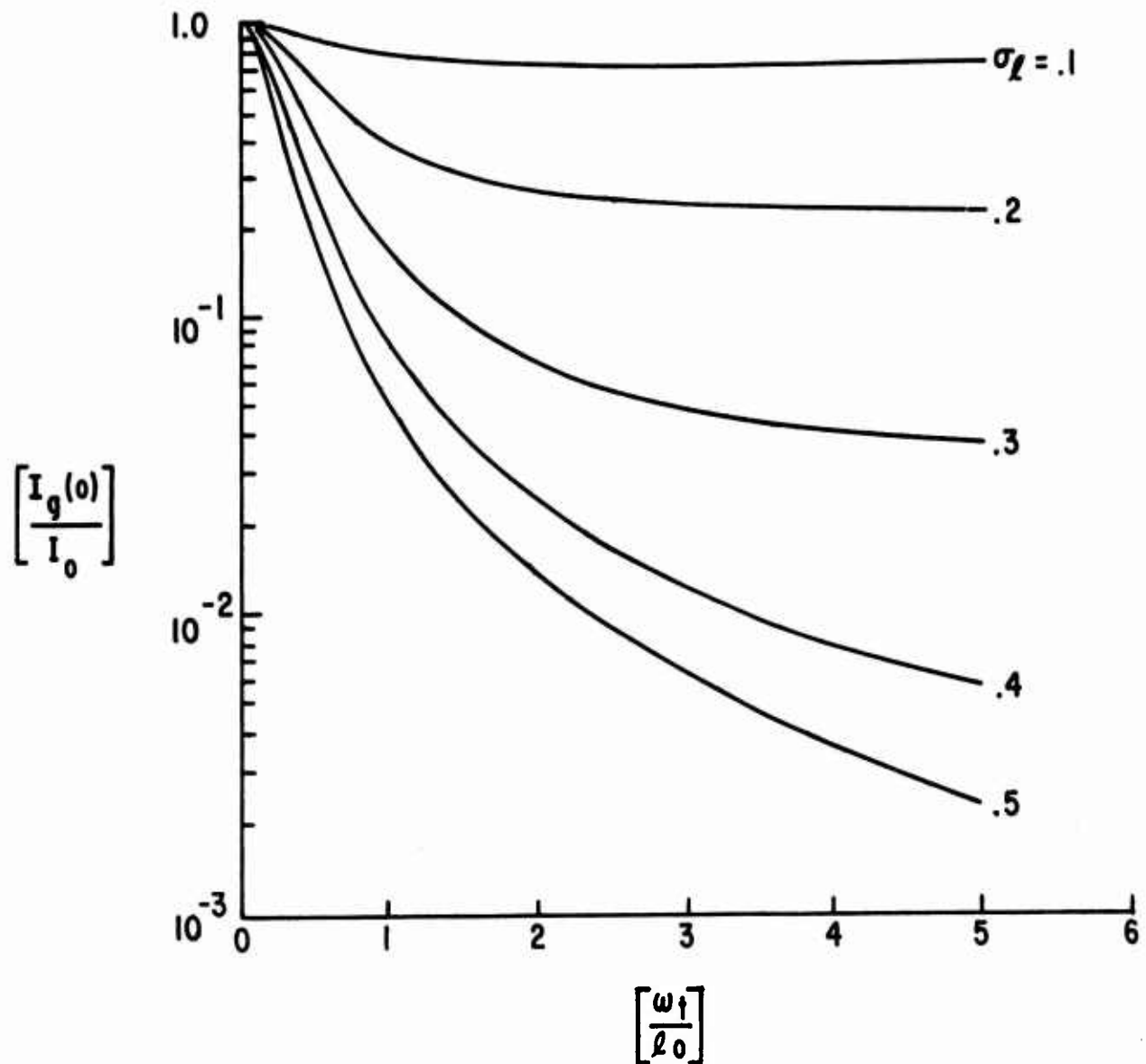


Figure 11. Reduction in Relative Maximum Average Irradiance Using the Modified Two Gaussian Beam Model with the Exact Calculation for the Scale Size L for Different rms Phase Distortions and Relative Correlation Lengths (ω_t/l_0)

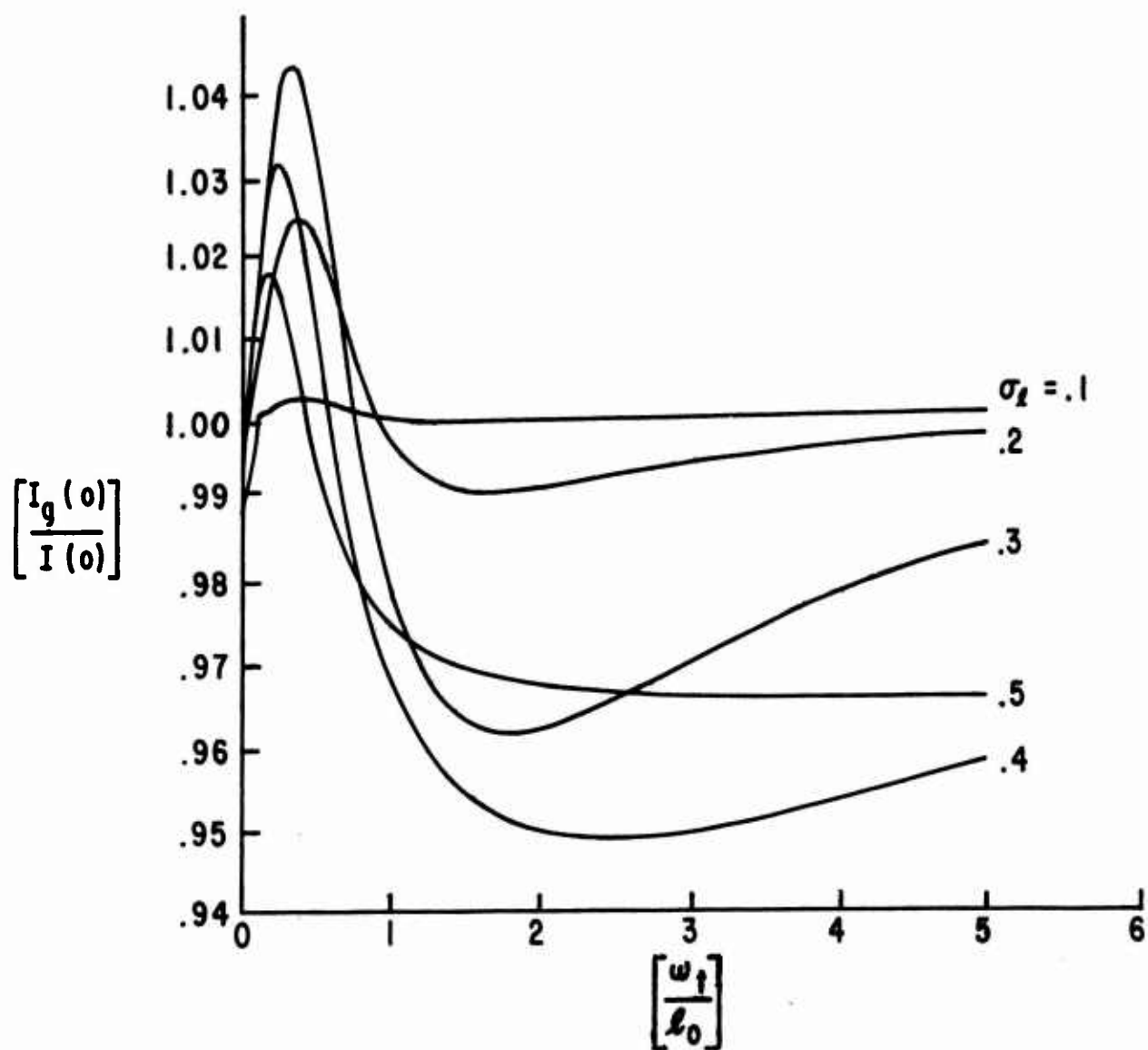


Figure 12. Ratio of the Exact Calculation for the Maximum Average Irradiance to the Modified Two Gaussian Beam Calculation as a Function of Phase Distortion (σ_l) and Relative Correlation Length (ω_t/ℓ_0)

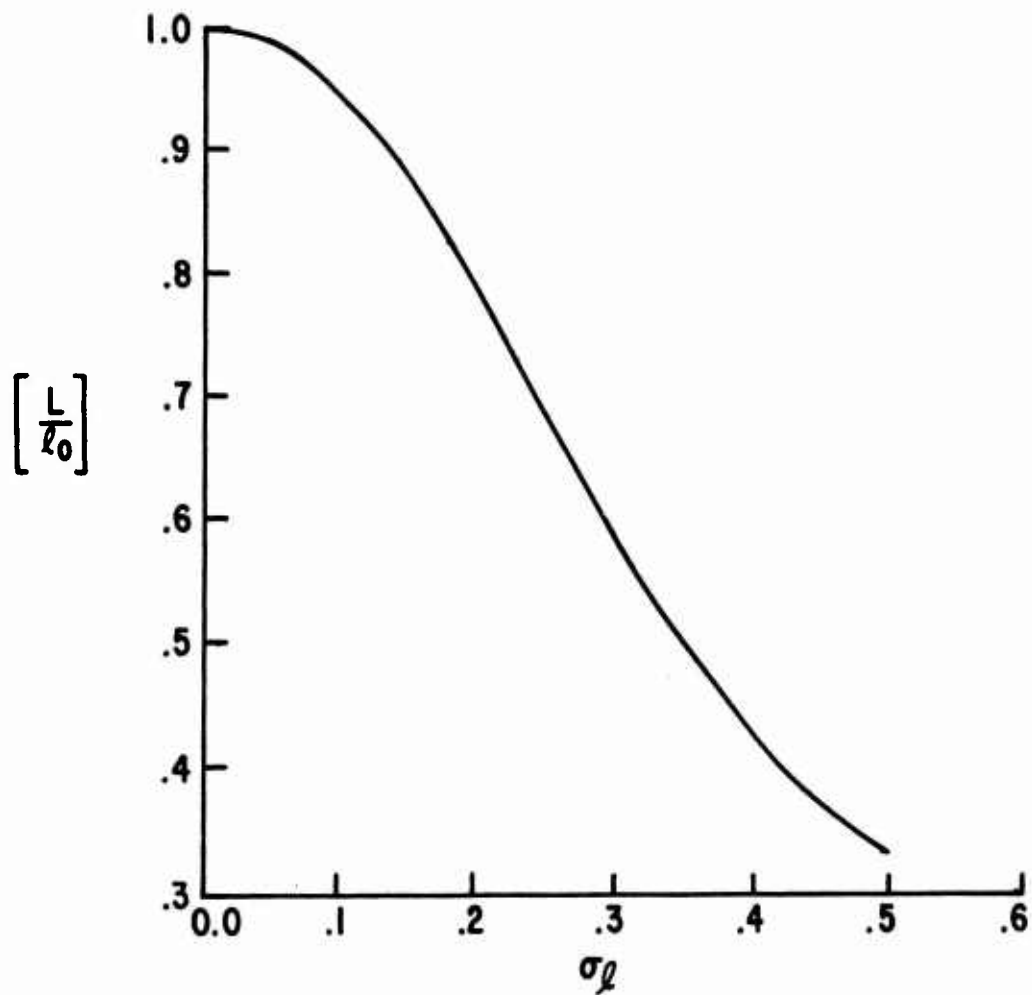
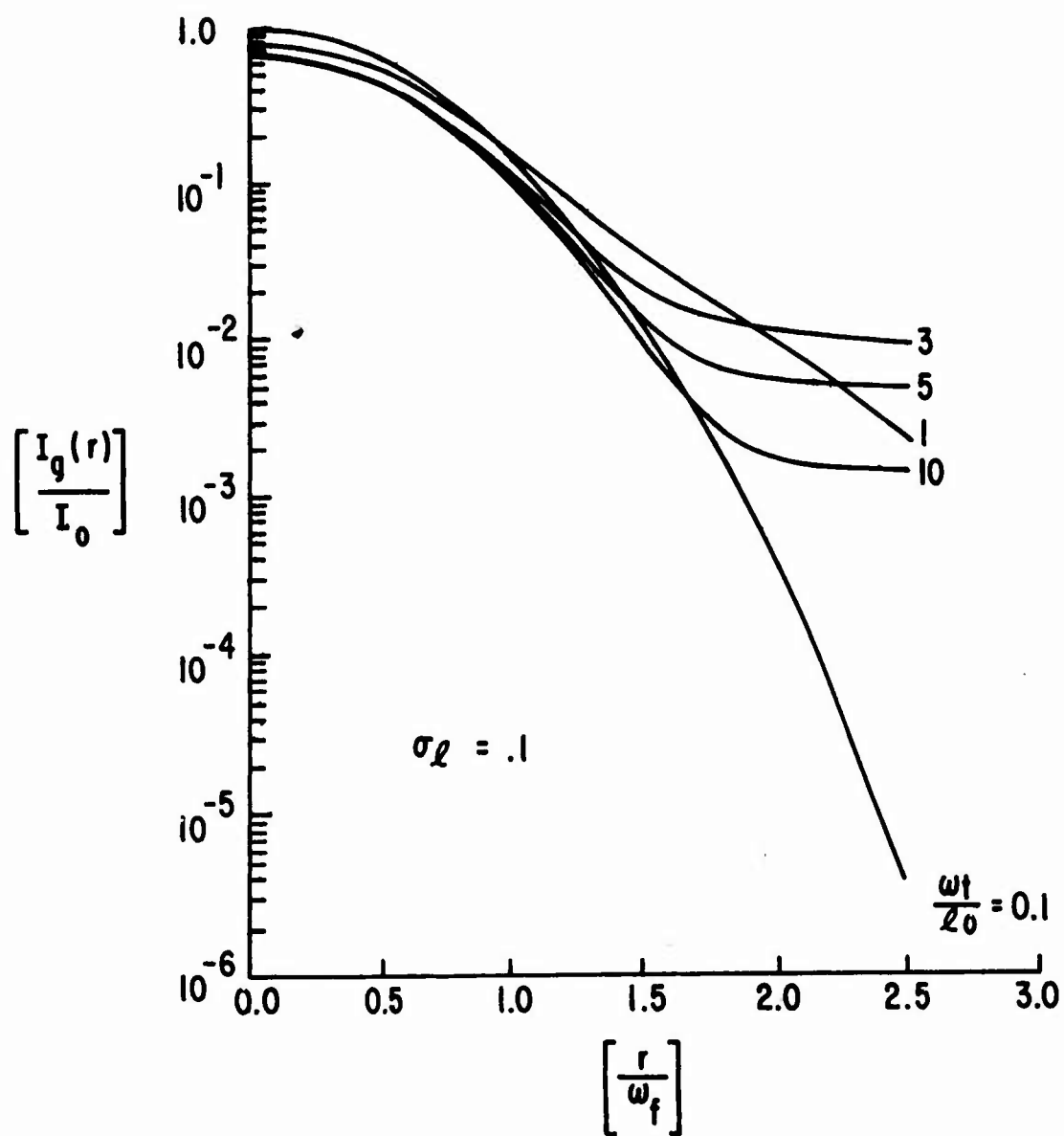


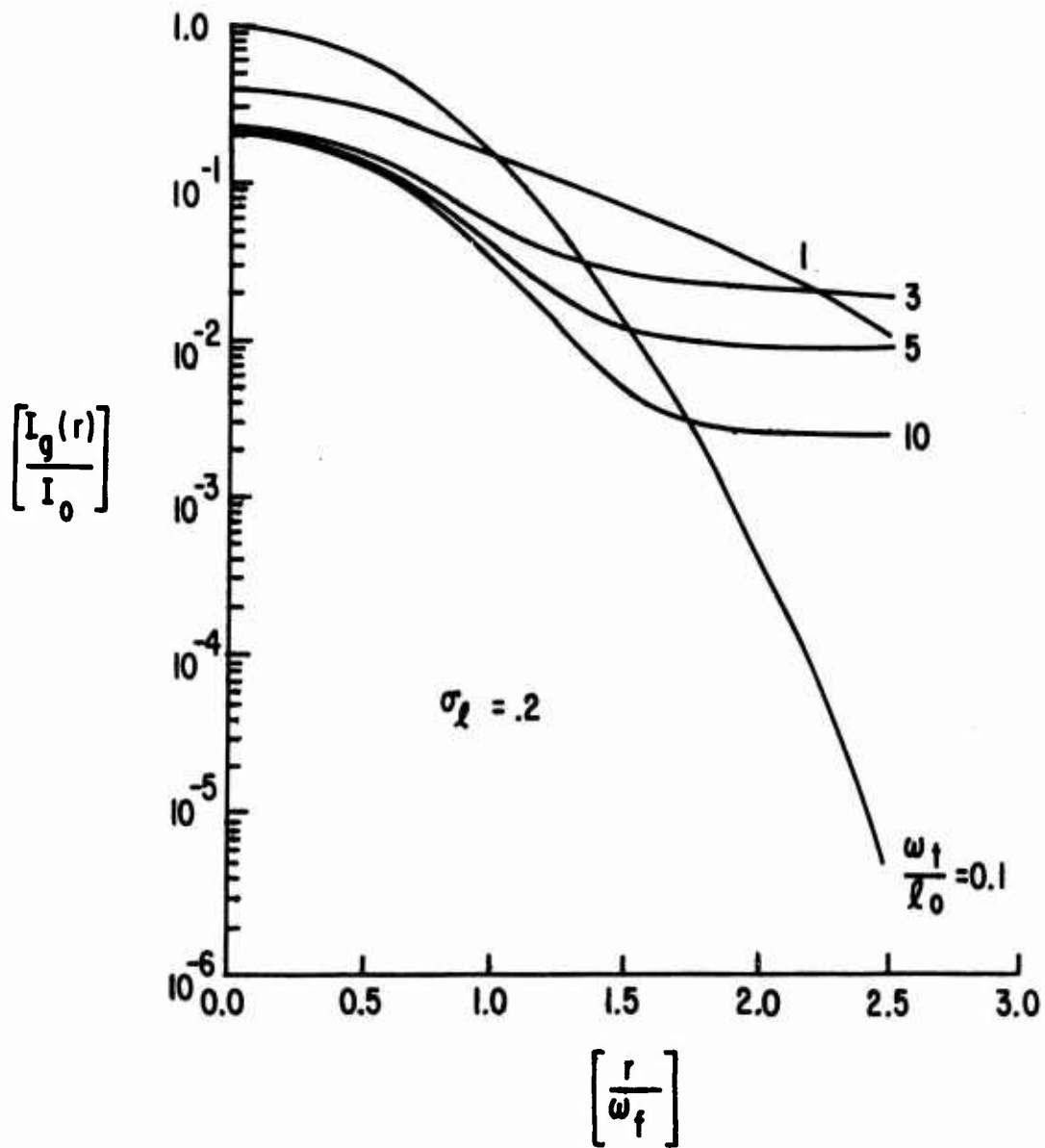
Figure 13. Dependence of Relative Scale Size (L/l_0) on the rms Phase Distortion σ_l

The spatial characteristics of this representation are shown in figures 14(a) through (e) and can be compared with the exact solution in figures 2(a) through (e). Again there is significant agreement between the two methods.



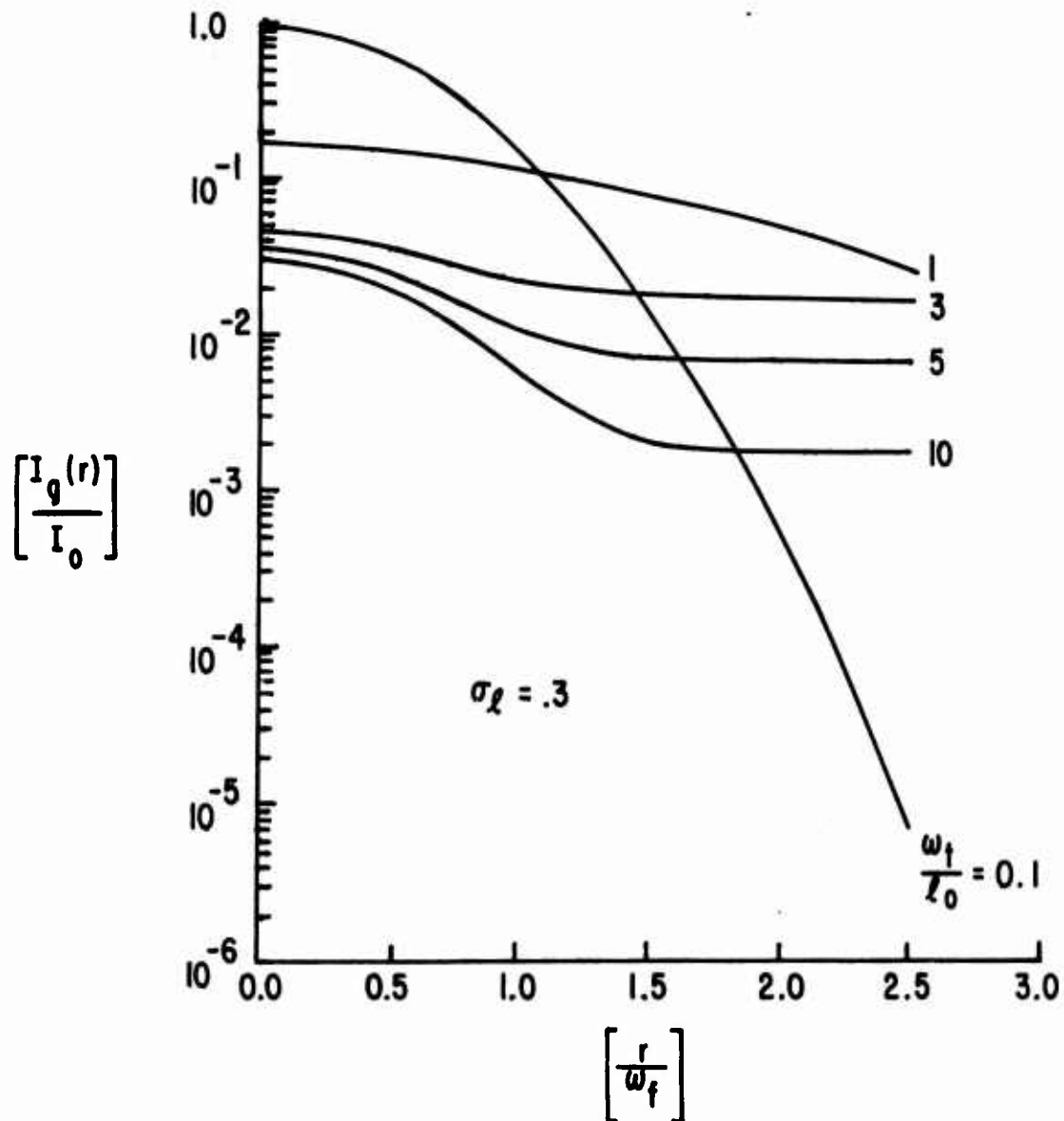
(a) $\sigma_L = 0.1$ wavelength

Figure 14. Relative Irradiance Profiles for Different Amounts of rms Phase Distortion and Relative Phase Correlation Length (ω_f/l_0) as Calculated Using the Modified Two Gaussian Beam Model



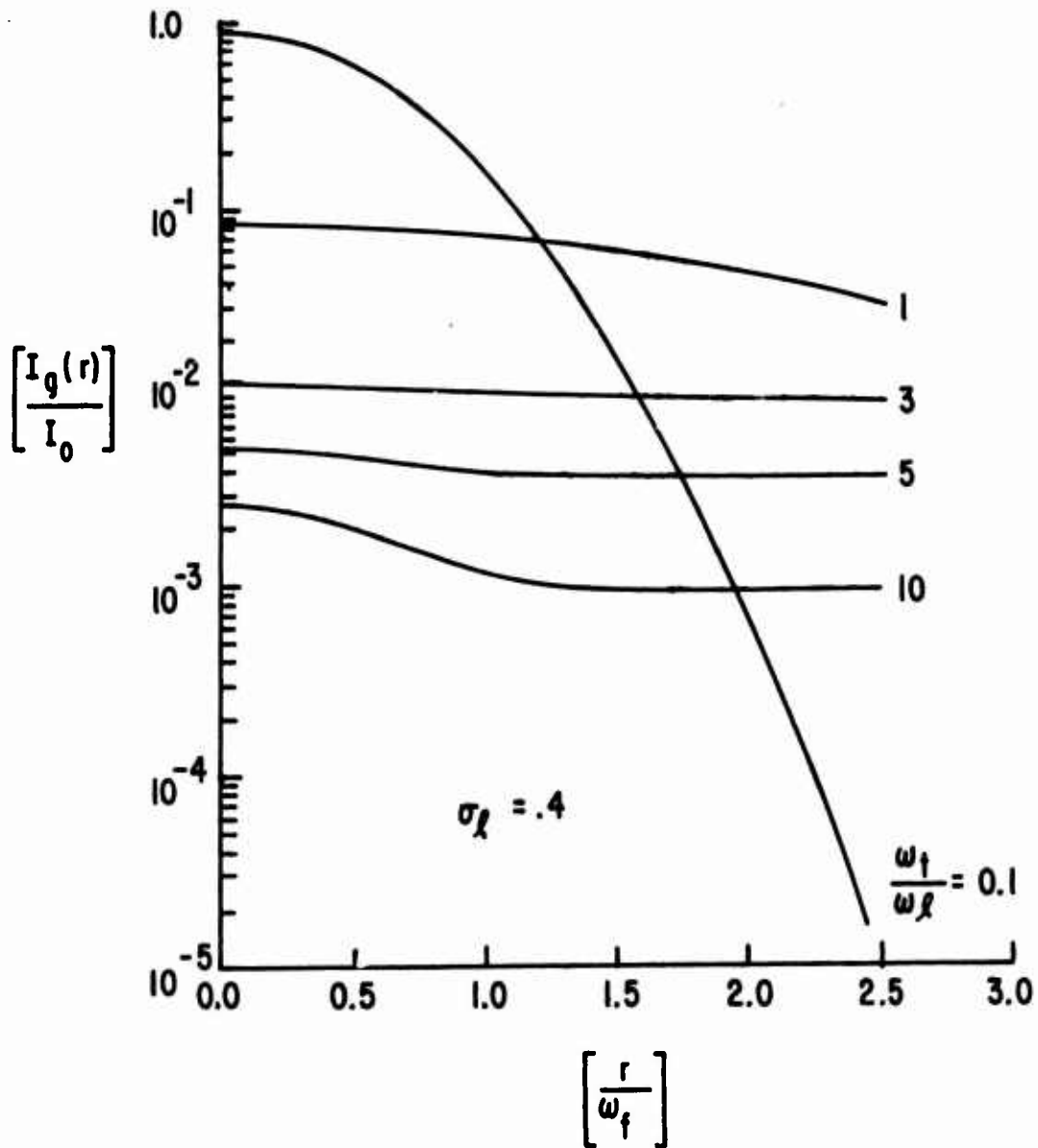
(b) $\sigma_\ell = 0.2$ wavelength

Figure 14. Relative Irradiance Profiles for Different Amounts of rms Phase Distortion and Relative Phase Correlation Length (ω_f/ℓ_0) as Calculated Using the Modified Two Gaussian Beam Model



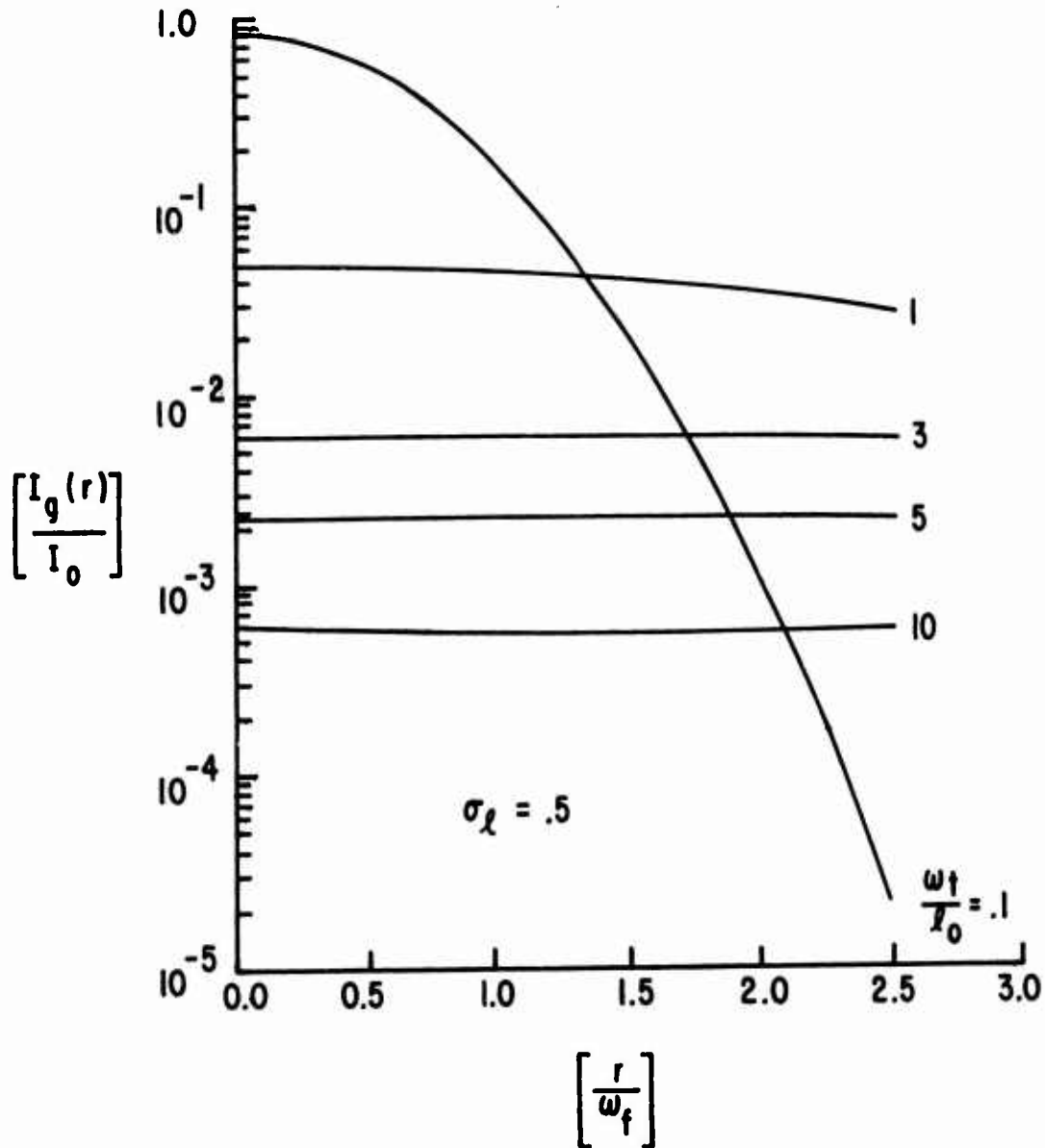
(c) $\sigma_l = 0.3$ wavelength

Figure 14. Relative Irradiance Profiles for Different Amounts of rms Phase Distortion and Relative Phase Correlation Length (ω_f/ω_0) as Calculated Using the Modified Two Gaussian Beam Model



(d) $\sigma_l = 0.4$ wavelength

Figure 14. Relative Irradiance Profiles for Different Amounts of rms Phase Distortion and Relative Phase Correlation Length (ω_f/ω_l) as Calculated Using the Modified Two Gaussian Beam Model



(e) $\sigma_\lambda = 0.5$ wavelength

Figure 14. Relative Irradiance Profiles for Different Amounts of rms Phase Distortion and Relative Phase Correlation Length (ω_f/λ_0) as Calculated Using the Modified Two Gaussian Beam Model

SECTION IV

SYSTEM JITTER AND CASCADED RANDOM PHASE DISTORTIONS

1. SYSTEM JITTER

Frequently, optical systems will contain sources of real random jitter. These can arise, for instance, from the telescope gimbals that control the pointing and tracking functions. Another source of beam jitter is mirror vibrations in optical trains.

While the preceding work investigated the optical distortions caused by random phase aberrations on diffraction limited beams, the inclusion of an inherent system jitter is very simple. The basic equation for the average irradiance distribution [equation (30) for the general case and equation (13) for the cause of a Gaussian beam] is modified in the following way

$$\langle I(x_0, y_0) \rangle = \int_{-\infty}^{\infty} \int_{-\infty}^{\infty} M_d(x, y) \cdot M_p(x, y) \cdot M_j(x, y) \exp \left[-i \frac{k}{f} (xx_0 + yy_0) \right] dx dy \quad (52)$$

where the MTF for simple jitter is

$$M_j(x, y) = \exp \left[- \frac{k^2 \overline{\theta_j^2}}{4} (x^2 + y^2) \right] \quad (53)$$

Particularizing to the case of an ideal Gaussian beam, the pertinent equations in the preceding sections must be revised as follows:

Define

$$\Omega^2 = (2 f^2 \overline{\theta_j^2} / \omega_f^2) \quad (54)$$

where ω_f is the diffraction limited focal plane spot size of the ideal Gaussian beam, f is the system focal length, and $\overline{\theta_j^2}$ is the one-sigma line-of-sight jitter. The equations (15), (21), (49) and (50) can be written as follows:

Equation (15):

$$\langle I(r) \rangle = \exp(-\sigma_\phi^2) I_0 \sum_{n=0}^{\infty} \frac{\sigma_\phi^{2n}}{n!} \left[\frac{1}{1 + \Omega^2 + 2nR^2} \right] \exp \left[\frac{-2r^2}{\omega_f^2} \frac{1}{(1 + \Omega^2 + 2nR^2)} \right] \quad (55)$$

Equation (21):

$$P(r) = P_0 \left[1 - \exp(-\sigma_\phi^2) \sum_{n=0}^{\infty} \frac{\sigma_\phi^{2n}}{n!} \exp \left[\frac{-2r^2}{\omega_f^2 (1+\Omega^2+2nR^2)} \right] \right] \quad (56)$$

Equation (49):

$$I_s(r) = (1 - \exp(-\sigma_\phi^2)) \cdot \left[I_0 \left(\frac{\omega_f^2 (1+\Omega^2)}{\omega_f^2 (1+\Omega^2) + 2\overline{\theta^2} f^2} \right) \cdot \exp \left[\frac{-2r^2}{\omega_f^2 (1+\Omega^2) + 2\overline{\theta^2} f^2} \right] \right] \quad (57)$$

where $\overline{\theta^2}$ is defined by equation (42).

Equation (50):

$$I_u(r) = \exp(-\sigma_\phi^2) \frac{I_0}{1+\Omega^2} \cdot \exp \left[\frac{-2r^2}{\omega_f^2 (1+\Omega^2)} \right] \quad (58)$$

The sensitivity of the results obtained in the previous sections on inherent system jitter can readily be studied with these few simple modifications.

2. CASCADED RANDOM PHASE DISTORTIONS

Many optical systems are composed of sequential optical components as well as environmental sources of optical distortions. Each component or process will have its own characteristics, and in the most general case, can present a formidable problem in the estimation of the total integrated system performance. If the sources of phase distortion are generated by independent random processes and if all parts of the entire optical train are well within the near-field of any of the phase distortions, then the average far-field irradiance distribution will be given by

$$\langle I(r) \rangle = \iint_{-\infty}^{\infty} M_d(\bar{r}) \cdot M_j(\bar{r}) \cdot \left(\prod_{n=1}^N M_n(\bar{r}) \right) \cdot \exp \left\{ -i \frac{k}{f} (xx_0 + yy_0) \right\} dx dy \quad (59)$$

where $M_j(\bar{r})$ is the jitter MTF, $M_d(\bar{r})$ is the diffraction limited MTF, and $M_n(\bar{r})$ ($n=1,2,\dots,N$) are the MTF's for the separate sources of optical phase distortion. Again, for a Gaussian random process,

$$M_n(\bar{r}) = \exp \left[-\sigma_{\phi_n}^2 + c_{\phi_n}(\bar{r}) \right] \quad (60)$$

Define an integrated system MTF as

$$M_S(\bar{r}) = \exp \left[\sum_{n=1}^N \sigma_{\phi_n}^2 + \sum_{n=1}^N c_{\phi_n}(\bar{r}) \right] \quad (61)$$

If the accumulated phase variance is less than a tenth of a wavelength, equation (60) can be expanded, resulting in a modified version of equation (4):

$$I_0(r) = \exp \left[\sum_{n=1}^N \sigma_{\phi_n}^2 \right] I_d(r) \quad (62)$$

$$I_1(r) = \exp \left(\sum_{n=1}^N \sigma_{\phi_n}^2 \right) \cdot \sum_{n=1}^N \int_0^\infty M_d(r_0) M_j(r_0) c_{\phi_n}(r) J_0 \left(\frac{kr_0 r}{f} \right) r_0 dr_0 \quad (63)$$

The irradiance distribution for the case of an initially Gaussian beam and the Gaussian covariance functions are then

$$\begin{aligned} \langle I(r) \rangle = & \exp \left[-\sum_{n=1}^N \sigma_{\phi_n}^2 \right] I_0 \left\{ \exp \left[-\frac{2r^2}{\omega_f^2} \frac{1}{(1+\Omega^2)} \right] \cdot \left(\frac{1}{1+\Omega^2} \right) \right. \\ & \left. + \sum_{n=1}^N \frac{\sigma_{\phi_n}^2}{(1+\Omega^2+2R_n^2)} \cdot \exp \left[-\frac{2r^2}{\omega_f^2} \cdot \frac{1}{(1+\Omega^2+2R_n^2)} \right] \right\} \end{aligned} \quad (64)$$

where $R_n = (\omega_t / \ell_{0n})$.

In terms of the approximate representation described in section III.2, a similar development can be pursued. The first order estimate for the Gaussian integral scale size [equation (46-b)] now becomes

$$L_1 = \frac{e^{-\frac{\sigma^2}{2}}}{1 - e^{-\frac{\sigma^2}{2}}} \cdot \sum_{n=1}^N \ell_{0n} \sigma_{\phi_n}^2 \quad (65)$$

where

$$\sigma^2 = \sum_{n=1}^N \sigma_{\phi_n}^2 \quad (66)$$

Extension of this approach, as well as the approach leading to equation (64) for higher order approximations, rapidly becomes cumbersome, and an alternate (but approximate) method described below may be more useful.

For convenience, assume that all the covariance functions of interest are Gaussian with variance $\sigma_{\phi_n}^2$ and correlation length ℓ_{0n} . In equation (61) the function defined here as

$$C(r) = \sum_{n=1}^N c_{\phi_n}(r) \quad (67)$$

resembles in some respects a covariance function itself. Its variance is given by equation (66), and as $r \rightarrow \infty$, $C(r) \rightarrow 0$. The shape of $C(r)$ as a function of r is not necessarily Gaussian, however. Nonetheless, an effective width of $C(r)$ can be defined. For convenience, again the integral scale size defined in equation (11) can be used and then $C(r)$ represented by a Gaussian covariance function, so that

$$C(r) \approx \sigma^2 \exp \left[-\frac{r^2}{(\bar{\ell})^2} \right] \quad (68)$$

where

$$\bar{\ell} = \frac{1}{\sigma^2} \cdot \sum_{n=1}^N \sigma_{\phi_n}^2 \ell_{0n} \quad (69)$$

The effective correlation length, $\bar{\ell}$, is seen to be an average of the individual correlation lengths, each weighted by its respective variance. Thus, for instance, if a process has a large correlation length, but a small variance, it contributes very little to the effective overall correlation length.

Definitions (68) and (69) can now be used to go through any of the preceding analyses. But it should be pointed out that the validity of this approach has not been tested. To do this would require a detailed analysis of many specific systems. Nonetheless, this approach does offer some insight into the dependence (and nature) of the system performance on different and discrete sources of optical distortions.

The assumed form of the covariance function [equation (68)] and the definition of the effective correlation length [equation (69)] should approximate the real situation quite well when the true covariance function $C(r)$ can be represented well by a single Gaussian function. There is a problem of practical importance, however, where this approach does not adequately represent the real situation. Consider figure 15. Suppose one source of phase aberrations is characterized by a very small correlation length ($\frac{\omega_t}{x_0} \gg 1$). It is depicted by $M_1(r)$ in figure 15. The second source of aberrations is assumed to have a large correlation length ($\frac{\omega_t}{x_0} \ll 1$), represented by $M_2(r)$ in figure 16. It is clear that the best representation of $M_S(r) = M_1(r) \cdot M_2(r)$ is simply $\exp(-\sigma_{\phi_1}^2) \cdot M_2(r)$. In other words, $M_1(r)$ is best interpreted as a source of energy extinction due to the wide angle scattering it engenders. Equation (69) will define an effective correlation length equal to

$$\bar{\ell} = \frac{\sigma_{\phi_1}^2 \ell_{01}^2 + \sigma_{\phi_2}^2 \ell_{02}}{\sigma_{\phi_1}^2 + \sigma_{\phi_2}^2} \approx \left(\frac{\sigma_{\phi_2}^2}{\sigma_{\phi_1}^2 + \sigma_{\phi_2}^2} \right) \ell_{02}$$

which for $\sigma_{\phi_2} \gg \sigma_{\phi_1}$ gives the result that $\bar{\ell} \approx \ell_{02}$. Clearly in this limit, no accounting whatsoever will be obtained for $M_1(r)$. The problem, of course, is that $M_S(r)$ in this instance cannot be represented very well by just a single Gaussian function of the form of equation (68).

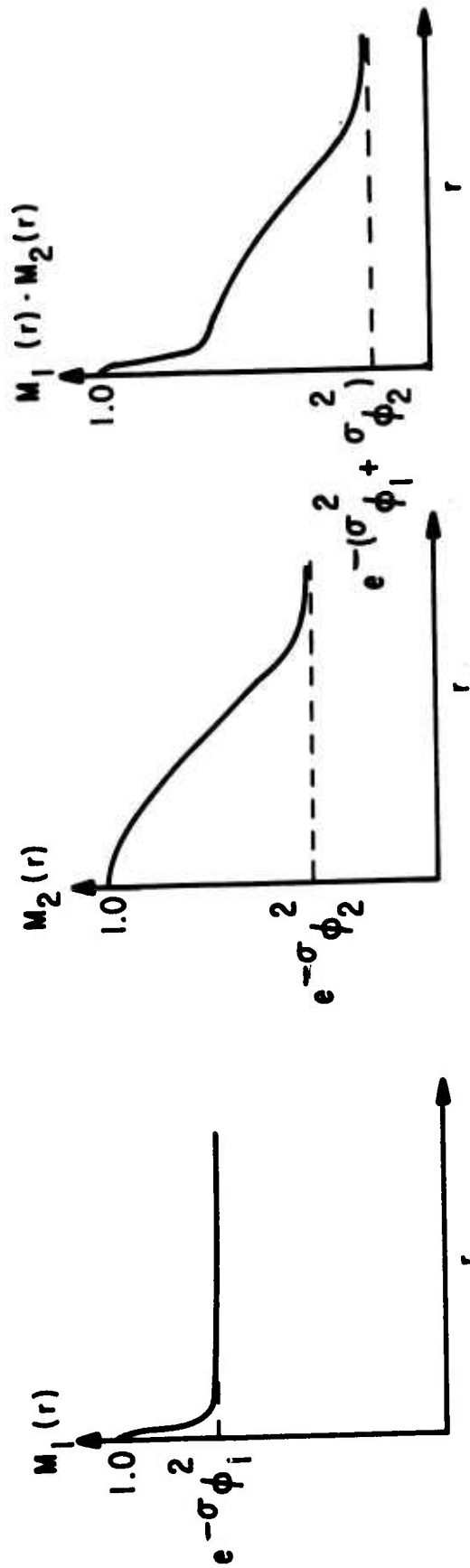


Figure 15. Cascaded MTF for Two Processes, One with a Very Small Phase Correlation Length and One with a Much Larger Correlation Length

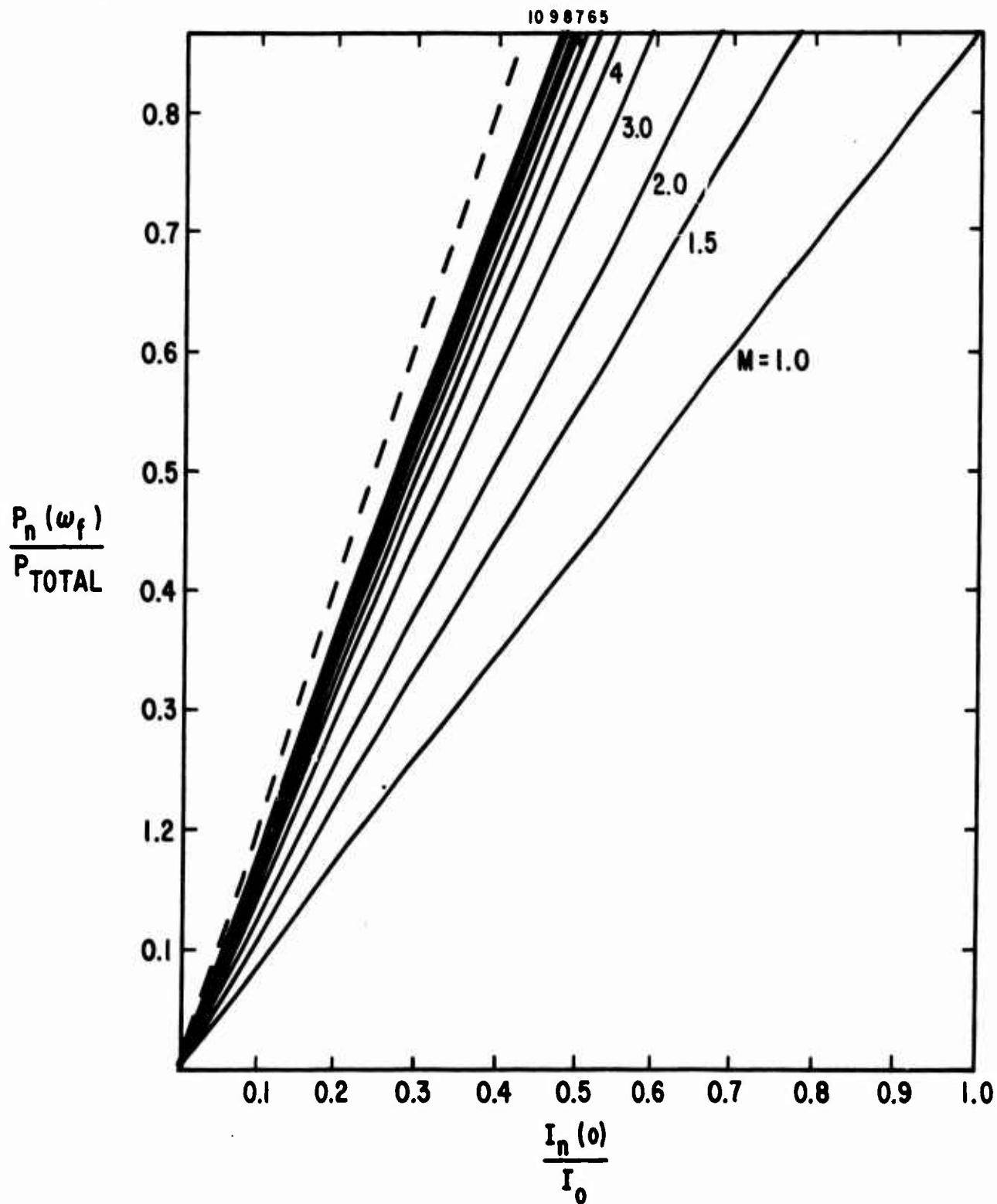


Figure 16. Parametric Dependence of M on the Relative Intensity Reduction and the Relative Integrated Power Decrease

SECTION V

OPTICAL SYSTEM MODELS

There are a number of computer models in use now that attempt to describe total high power system performance characteristics in a consistent and integrated fashion. Necessarily, by the magnitude and complexity of such a problem in the development of these codes, the designers have had to make numerous simplifying assumptions. One frequently used approach, for instance, is to approximate the focal plane irradiance distribution of the diffraction limited system by a Gaussian beam, with a modified amplitude and spot size (ref. 4). Most optical systems, however, operate with less than ideal amplitude and phase output characteristics. The corresponding focal plane irradiance distributions are therefore less than diffraction limited as evidenced by reduced peak intensity and spot spreading. For small scale phase aberrations, wide angle scattering effectively removes a fraction of the usable energy from the far-field spot. Larger scale phase aberrations reduce the maximum irradiance by spreading the beam.

Whether the actual focal plane distribution of the beam is spread or widely scattered depends, of course, on the nature of the output aberrations, and for any given situation, it is reasonable to say that both spreading and scattering will be present simultaneously. In general then, far-field patterns, such as the one shown in figure 9, may be more characteristic of actual random phase aberrated beams.

The formalism developed in section III.2 described the nondiffraction limited beam as the sum of two beams. For the case of a transmitted Gaussian beam, the two focal plane beams were found to also be Gaussian in shape (figure 9). Thus, for purposes of computer modelling, perhaps two Gaussian beams, instead of one, could be incorporated into the system description. The given information on the variance and correlation length of the phase distortions could then be used to construct the appropriate far-field beam model required in the calculation.

Because this may not be a convenient or easy modification to pursue, the

4. Peckham, L.N., and Davis, R.W., AFWL-TR-72-95, Air Force Weapons Laboratory (Rev.)

next question is how can a profile such as that shown in figure 9 be approximated by a single Gaussian function. In spite of the shortcomings of this approach, something like the following could be attempted.

Define a Gaussian beam to be used for the model as

$$I_g(r) = \frac{m_1 I_0}{m_2^2} \exp\left(-\frac{2r^2}{m_2^2 \omega_f^2}\right) \quad (70)$$

where m_1 is a parameter used to describe the amount of energy lost to wide angle scattering, and m_2 is a parameter used to describe the spread of the beam relative to the diffraction limited spot size given by ω_f . When $m_1 = m_2 = 1$, the beam is diffraction limited. If the scale size of the phase fluctuations is much less than the diameter of the transmitting aperture, then all the energy will be scattered "out" of the main beam. In this situation, the nondiffraction limited parameters would be specified as

$$m_1 = \exp(-\sigma_\phi^2) \quad (71-a)$$

$$m_2 = 1.0$$

If the scale size of the phase distortions is large compared to the transmitting aperture, then the far-field pattern resembles the pattern of a beam that has been distorted by simple jitter [see equation (22)]. For this extreme case, the nondiffraction limited parameters should be specified as

$$m_1 = 1$$

$$m_2 = \frac{\omega_f'}{\omega_f} \quad (71-b)$$

when $(\omega_f')^2 = (\omega_f^2 + 2 f^2 \overline{\theta^2})$ is the spot size of the spread beam.

Specification of m_1 and m_2 for these two special limiting cases is straightforward. This was made true by virtue of the fact that in each case the beam was still Gaussian in shape. For the multitude of cases that lie between these extremes, the irradiance profile will not be Gaussian. The question becomes, how can a single Gaussian profile represent this in a manner that

recognizes the important beam characteristics. Two parameters of interest that often are used to describe beam properties are the on-axis intensity and the integrated energy contained in a bucket of some specified radius. Let $I(0)$ and $P(\omega_f)$ represent these two quantities. They can be determined either from a theoretical calculation or, if experimental data are available, from specific far-field beam measurements. In terms of equation (70), then, the two resulting equations are

$$\frac{I(0)}{I_0} = \frac{m_1}{m_2^2} \quad (72)$$

$$\frac{P(\omega_f)}{P_0} = m_1 \left(1 - \exp(-2/m_2^2) \right) \quad (73)$$

where the bucket radius used for the power equation was ω_f . Defining $m_2^2 = M$, it is easy to show that the following transcendental equation can be obtained.

$$\frac{P(\omega_f)}{P_0} \cdot \frac{I_0}{I(0)} = M \left(1 - \exp - \frac{2}{M} \right) \quad (74)$$

Equation (74) will obtain a solution only when $\frac{P(\omega_f)}{P_0} \cdot \frac{I_0}{I(0)} < 2$. Figure 16 enables M to be determined after $\left(\frac{P(\omega_f)}{P_0} \right)$ and $\left(\frac{I(0)}{I_0} \right)$ have been specified. Once

M has been determined, then

$$m_1 = \frac{I(0)}{I_0} \cdot M \quad (75)$$

$$m_2 = +\sqrt{M}$$

It is easy to show that this definition of the Gaussian function (equation 70) reduces to the two extreme cases described earlier.

Figure 17 shows the results of representing the actual nondiffraction limited beam profile as (1) a pure energy extinction due to wide angle scattering, (2) a simple smearing of the energy due to jitter-like distortion, and

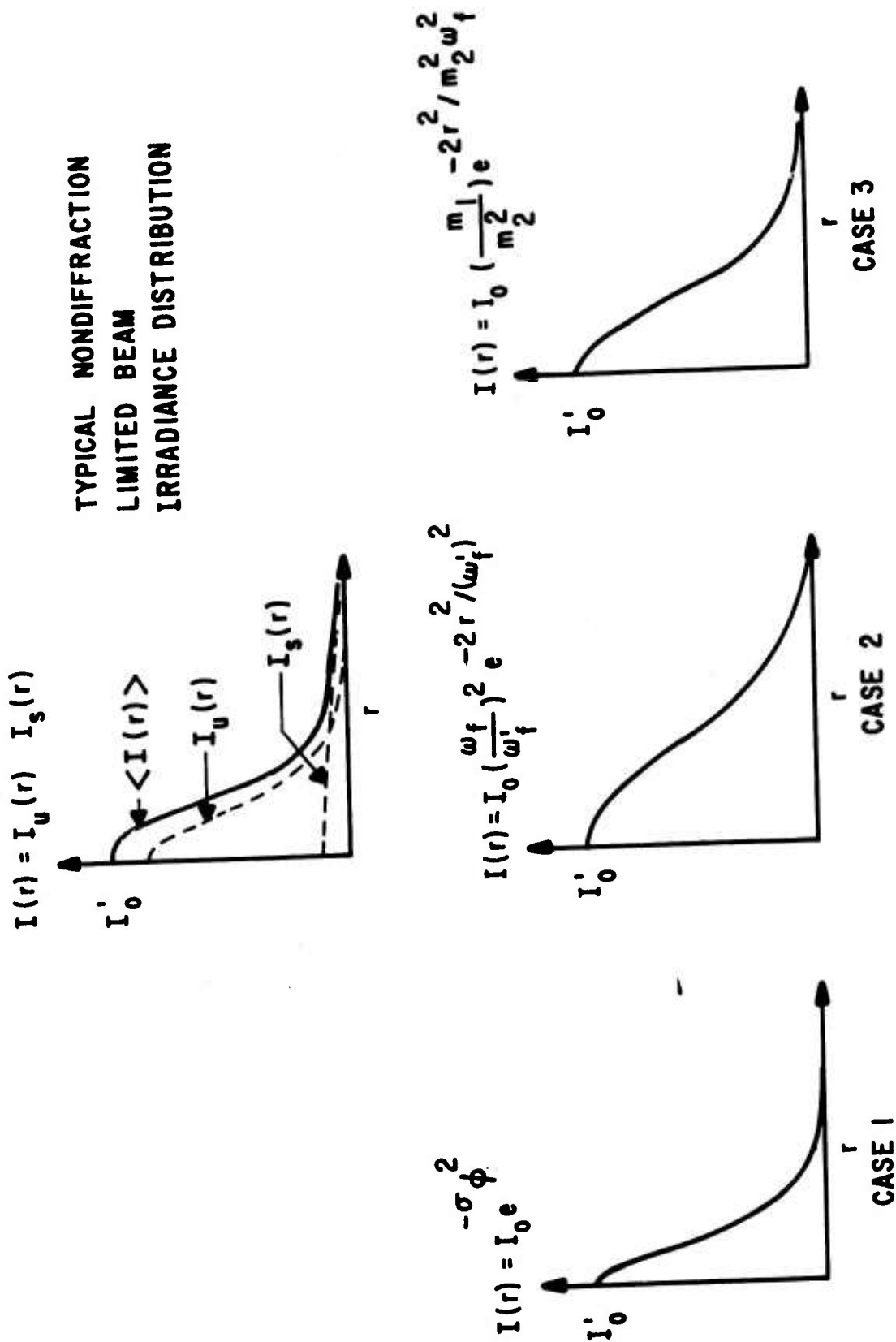


Figure 17. Three Approximations to the Nondiffraction Limited Beam

(3) the combination of scattering and spreading given by equation (70). The latter representation is seen to fall between cases (1) and (2).

Equation (70) is only an approximate representation of a more complex irradiance pattern. However, it does provide a model for the focal plane irradiance distribution that is consistent with two characteristics that are often used to quantitatively describe high energy laser systems, the peak intensity, and the energy contained in a standard sized radius bucket. These quantities could be obtained either from the analytic results of the approaches described in sections II through IV or from experimental measurements taken directly on real laser systems. A minimum adjustment is required to implement this model in most of the existing system codes available now.

SECTION VI

CONCLUSIONS

Most optical systems have performance characteristics that are less than diffraction limited. To model these systems, one needs to study the effect of random aberrations on the focal plane irradiance characteristics. The aberrations can arise from either random phase or random amplitude distortions. While both sources of error are usually present in optical systems, it can be shown that phase aberrations usually produce the most serious far-field distortions. This report has addressed the effect of random phase distortions on the focal plane characteristics of optical systems.

Consider a process that produces random phase distortions over an aperture of an optical system. Assume that the process is stationary in time and is spatially homogeneous and isotropic. Further assume that the quantities of interest are the average spatial characteristics of the far-field irradiance distribution. Then the statistical nature of the process can be approximately characterized by its mean (which is independent of \vec{r}) and by its covariance function (which is a function only of spatial separation in the aperture plane). For convenience, the system is assumed to be aligned so that the mean $\bar{\phi} = 0.0$. Then, the average far-field irradiance distribution is completely characterized by the spatial covariance function $C_{\phi}(r)$ of the phase fluctuations.

$C_{\phi}(r)$ can be any function that represents a physically realizable random process. While this places some constraints on the nature of the function, its actual shape can vary markedly. Nonetheless, some characteristics must always be present. For one thing, $C_{\phi}(0) = \sigma_{\phi}^2$ is the variance of the phase fluctuations. Also, as $r \rightarrow \infty$, $C(r) \rightarrow 0$, though not necessarily monotonically. To illustrate the qualitative nature of the processes being studied, however, it was convenient to specify a particular form for this function. For this report, a Gaussian covariance function was assumed, which of course implies that the spatial power spectrum of the phase fluctuations is also Gaussian in shape. While this diminishes the generality of this report, the qualitative dependence of the results for the average focal plane irradiance distribution still exhibits its characteristic dependence on the parameters of interest, the phase variance (σ_{ϕ}^2) and correlation length (ℓ_0). This is true despite the fact that

the form of the nonaberrated beam was often taken to be Gaussian in shape in order to facilitate numerical results. The conclusions inferred by these results should still be appropriate to the more general problem of arbitrary optical system characteristics and arbitrary random phase aberrations. The salient conclusions of this report then are the following:

a. When the rms phase distortion is less than 0.1 wavelength, the average far-field relative maximum irradiance is not altered substantially by including the effect of a non-zero phase correlation length, though the complete irradiance profile does show a marked difference in shape as when going from a very large correlation length ($\ell_0 \gg \omega_t$) to a very small one ($\ell_0 \ll \omega_t$). Nonetheless, for $\frac{\omega_t}{x_0} > 10$, only second order changes occur in the average relative focal plane irradiance distribution. Thus using equation (3) probably gives a very good representation of the far-field distribution.

b. When the rms phase is greater than 0.1 wavelength, the relative size of the phase correlation length to the effective aperture diameter is very important in determining the maximum average intensity, as well as the entire shape of the irradiance profile. Nonetheless, for $\sigma_\ell < 0.4$ wavelength, and $\frac{\omega_t}{x_0} > 2.0$, a very good estimate can still be obtained for the maximum average irradiance by again using equation (3). Thus when the scale length of the phase distortions is less than one-fourth the diameter of the transmitting aperture, the physical process seems to be dominated by wide angle scattering. The conclusion is that equation (3) represents the results of the physical process quite well over a wide range of values of σ_ℓ and ℓ_0 , but when these conditions are violated, the maximum relative irradiance dependence on the relative phase scale size can be very severe. These results are of particular importance to physical processes that scale with wavelength, so that σ_ϕ^2 [equations (1) and (2)] will be larger for shorter wavelength systems. Localized random index of refraction fluctuations that can be treated as a thin phase screen are an example. As such, systems operating at shorter optical wavelengths will be more apt to require the full analysis described in this report.

c. Attempting to account for the effects of the finite phase correlation length by using equation (4) does not gain a significant improvement in the estimate of the far-field maximum average intensity when $\sigma_\ell < 0.3$ and $\frac{\omega_t}{x_0} > 2$,

though some improvement is observed for $\frac{\omega t}{x_0} < 2$, then $\sigma_x < 0.2$ (figures 4 and 5). Nonetheless, the degree of improvement probably does not warrant the use of the second term in equation (4). In addition, this approach does not conserve energy nor does it provide a useful way of visualizing the characteristics of the physical process.

d. The two (Gaussian) beam model described in section III.2 accurately represents the exact analysis, and furthermore it provides an easy way to obtain good estimates of the reduction in maximum irradiance and profile characteristics. This approach can provide a possible system modelling scheme that would include the effects of finite phase scale lengths under the conditions of strong phase distortion.

e. In lieu of a two beam approach, systems codes could use a model described by equation (70). Though this form is not exactly correct, it does provide the user with a means of at least satisfying the two of the frequently used characteristics of nondiffraction limited beams; namely, reduction in peak intensity and power in a bucket. Nonetheless, the shortcomings of this approach should always be considered.

f. Inclusion of system jitter and multiple source aberrations have been demonstrated to be a relatively simple problem. With some caution, the approximate two beam approach described in section IV.2 is probably the easiest to implement, and in addition, it provides a useful insight into the dependence of the final result on the respective sources of aberrations.

In conclusion, the analysis of optical systems with strong random phase aberrations requires special attention to the phase correlation size. This means that particular attention may have to be given to systems operating with shorter wavelength radiation. This report has addressed some of these questions.